Towards Efficient Aero-Structural-Acoustic Optimization for Urban Air Mobility Vehicle Design

Bernardo Pacini

MDO Lab – Prof. Joaquim R. R. A. Martins

CAS Lab – Prof. Karthik Duraisamy

Oct. 25th, 2022 Tue

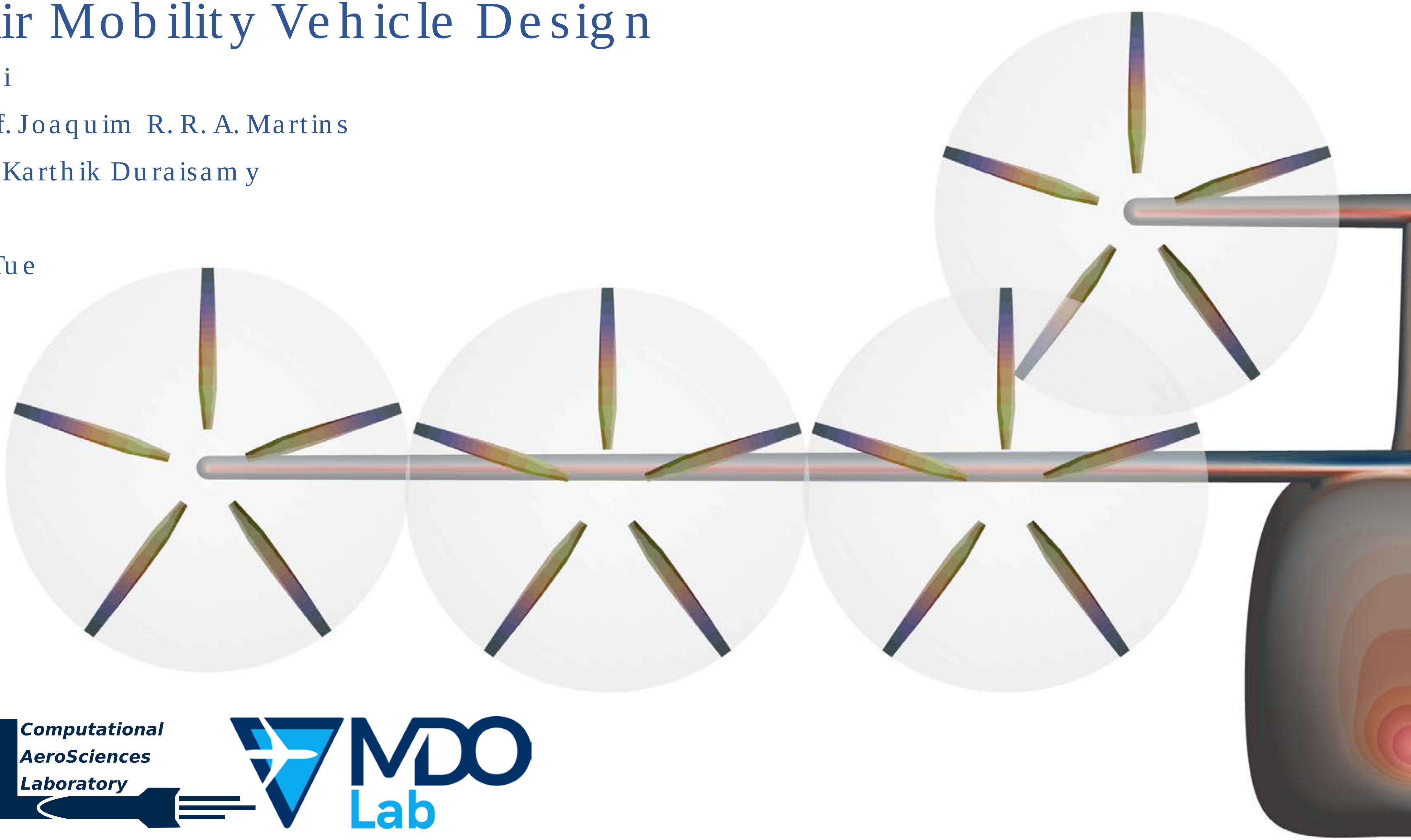

Computational AeroSciences Laboratory

MDO Lab

What is UAM?

- Urban Air Mobility (UAM) is a field that aims to improve movement of people and goods within cities by relieving congestion within transportation networks

- Facilitated by:

    1. Distributed electric propulsion

    2. Autonomous Technologies

www.nasa.gov

What does a UAM vehicle look like?

Joby
https://www.theverge.com/2020/1/15/21068135/joby-aviation-toyota-flying-air-taxi-investment-amount

Archer
https://www.bloomberg.com/news/articles/2021-06-11/electric-flying-taxi-backed-by-united-airlines-unveiled-in-l-a

Hyundai
https://www.adweek.com/brand-marketing/uber-chooses-hyundai-to-build-its-air-taxi-fleet/

Beta
https://evtol.news/beta-technologies-alia/

Wisk
https://www.autofutures.tv/2020/04/17/wisk-and-returns/

Volocopter
https://evtol.news/volocopter-volocity/

Ten Areas of Technological Development

Ease of Certification

Affordability

Safety

Ease of Use

Door to Door Speed

Average Trip Speed

Community Noise

Efficiency

Ride Quality

Lifecycle Emissions

Significant Technological Barriers to Development

K R Antcliff, S K S Whiteside, L W Kohlman, and C Silva. Baseline Assumptions and Future Research Areas for Urban Air Mobility Vehicles. In AIAA Scitech 2019 Forum, pages 1–18, San Diego, California, 2019.

How can OpenMDAO help solve the noise problem?

UAM Vehicle Design Process

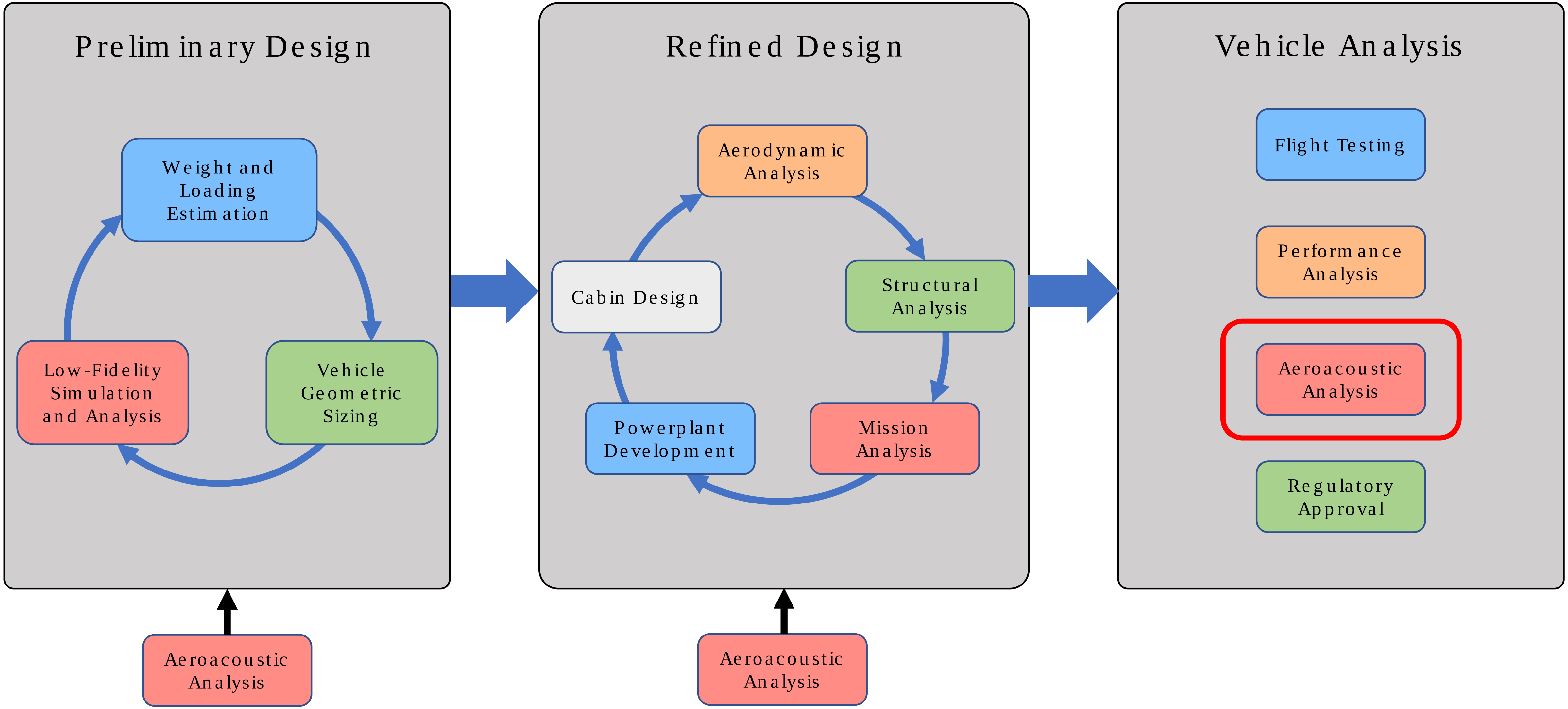

What type of work does the MDO Lab do?

In the MDO Lab:

Wing span

Airfoil shapes

Structural sizing

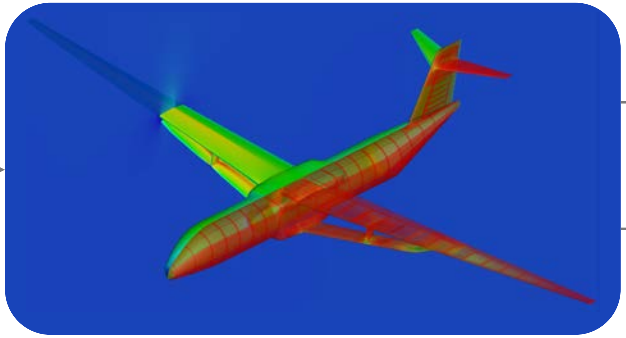

Fuel burn

Structural stresses

Design changes

minimize	f(x)	objective
with respect to	x	design variables
subject to	$c(x) \le 0$	constraints

- Electro-propulsive design optimization

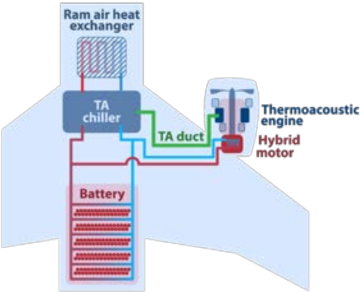

- Aerodynamic optimization with packaging

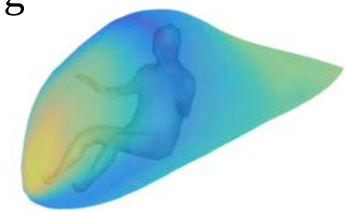

- Aero-propulsive design optimization

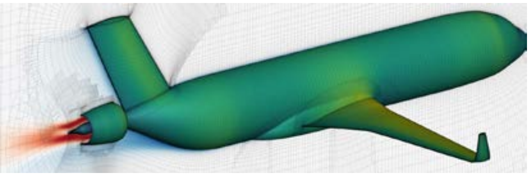

- Trajectory optimization

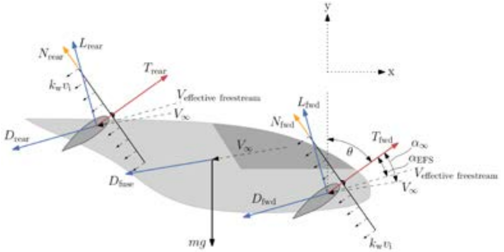

- Aero-thermal shape optimization

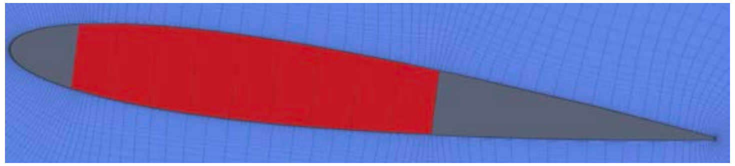

Slide adapted from: *Martins et al, Exploiting Aircraft Electrification via Multidisciplinary Design Optimization*

Why do I care about MDO?

- Electric vehicles are highly-coupled systems that must be designed and optimized considering all aspects of the vehicle and configuration

Table 5
Electric aircraft modeling and simulation [164].

	GT-HEAT [142,154,164]	NASA X-57	NASA N-3X	ESAero [67]	Bauhaus Luftfahrt
Aerodynamics	FLOPS/drag polar; BLI benefit based on flat-plate momentum thickness	Design using vortex lattice/ boundary layer codes; some CFD for analysis [51,85,158]	CFD results from similar configuration, with increment for BLI [56]	Drag polar	L/D correction methods from Torenbeek [16]
Structures	NA	6 DOF beam FEM [158]	NA	NA (for MDAO); detailed analysis of split-wing published in NASA report	NA
Weights	FLOPS tops-down methods	Parametric wing weight (from Raymer) [51], sized beam model [158]	WATE for propulsion flowpaths; tops-down kg/kW estimates for electrics/TMS [90,91]	WATE for fan weight [81]; low-fidelity radiator model; tops-down empirical for all others	Semi-empirical structural methods; tops-down kg/kW methods for electrics [20]
GNC	Engine, motor, TMS control variables for on- and off-design analysis	Full-mission optimal control [141]	NA; some discussion of off-design conditions in [57]	NA	NA
Electrical	Moderate fidelity motor/ inverter loss modeling; equivalent-circuit battery	Transient battery model based on Thevenin equiv. circuits (cell-level). Assumed efficiencies for wire/motors [141]	Conceptual: efficiency stackup method with estimates for future tech. Transient: RLC circuit model in SimPowerSystems [90,95]	Efficiency stackup; battery model unclear	Low-fidelity efficiency stackup with empirical battery discharge curve [20]
Turbo/Propulsion	NPSS	Propeller map from manuf.; prop efficiency from theory [141], blade element momentum theory [158]	NPSS [59]	2D fan analysis using velocity triangles [81]; efficiency maps for turbomachinery	Single prop efficiency parameter [20]
Thermal	TMS sizing considering various heat sources and types of heat sinks	Analytical model for optimization; thermal FEM of motor [141,153]	Coolant system load based on efficiency stackup (assume 100% to heat) [90]	Cooling based on flight cond. [79]; TMS model discussed in [119]	NA
Cash operating cost	NA except for fuel/energy	NA except for fuel/energy	NA	NA	Considers relative cost of fuel/elec; cash operating cost [25]
Ownership cost	NA	NA	NA	NA	NA
Noise	NA	NA	ANOPP noise simulation prompted redesign [91]	NA	NA
Safety	NA	Comprehensive FMEA [52,53]	FMEA and FTA for loss of thrust; more work needed for other hazards [94,96]	Qualitative	NA

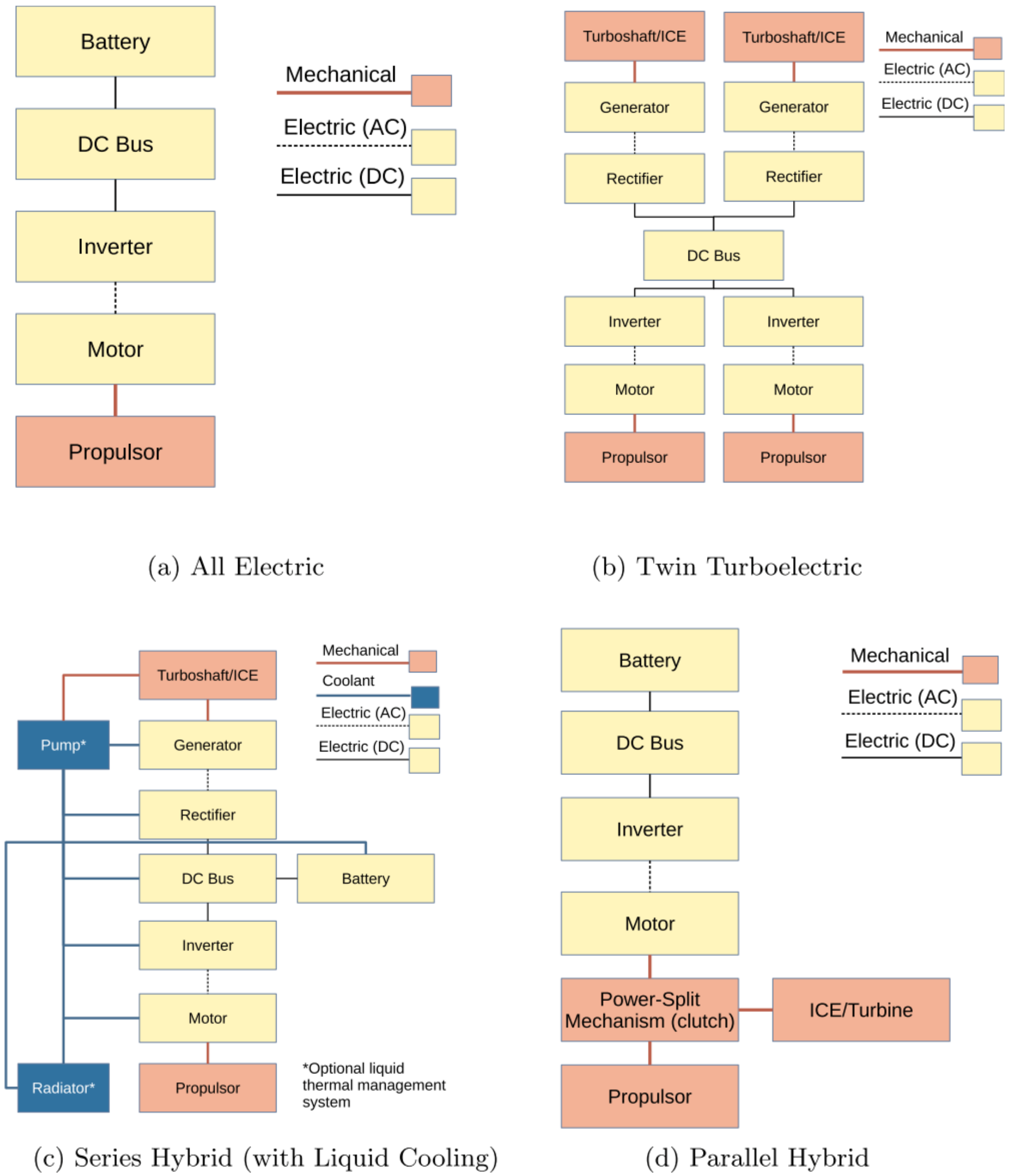

Fig. 2. Notional electric propulsion architectures.

Reproduced from: Brelje & Martins, Electric, hybrid, and turboelectric fixed-wing aircraft: A review of concepts, models, and design approaches

Why do we need gradients specifically?

Gradient Free Methods

Gradient Based Methods

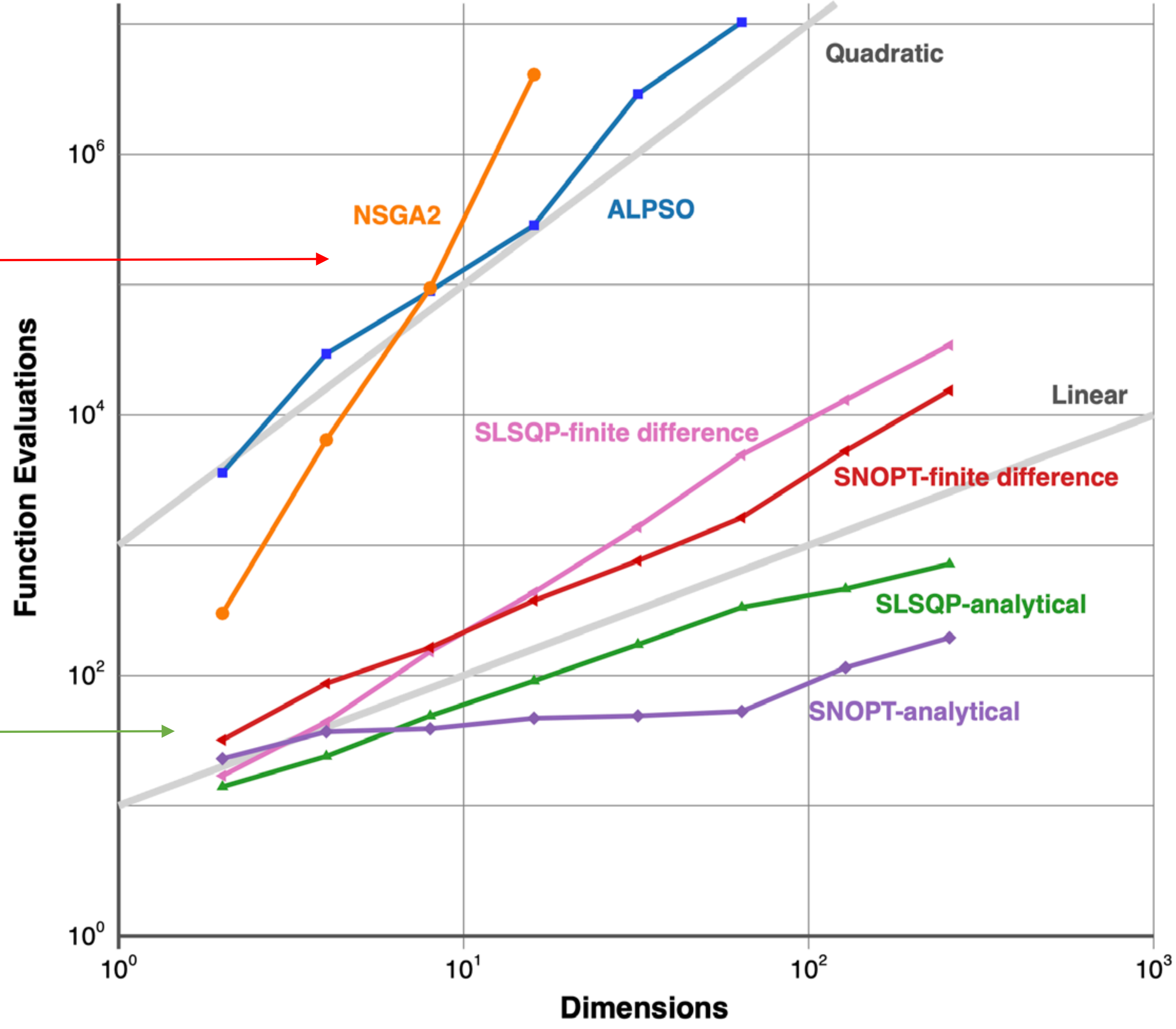

Lyu, Xu, and Martins. Benchmarking optimization algorithms for wing aerodynamic design optimization. ICCFD8-2014-0203.

Coupled Aerodynamic and Aeroacoustic Optimization

eXtended Design Structure Matrix:

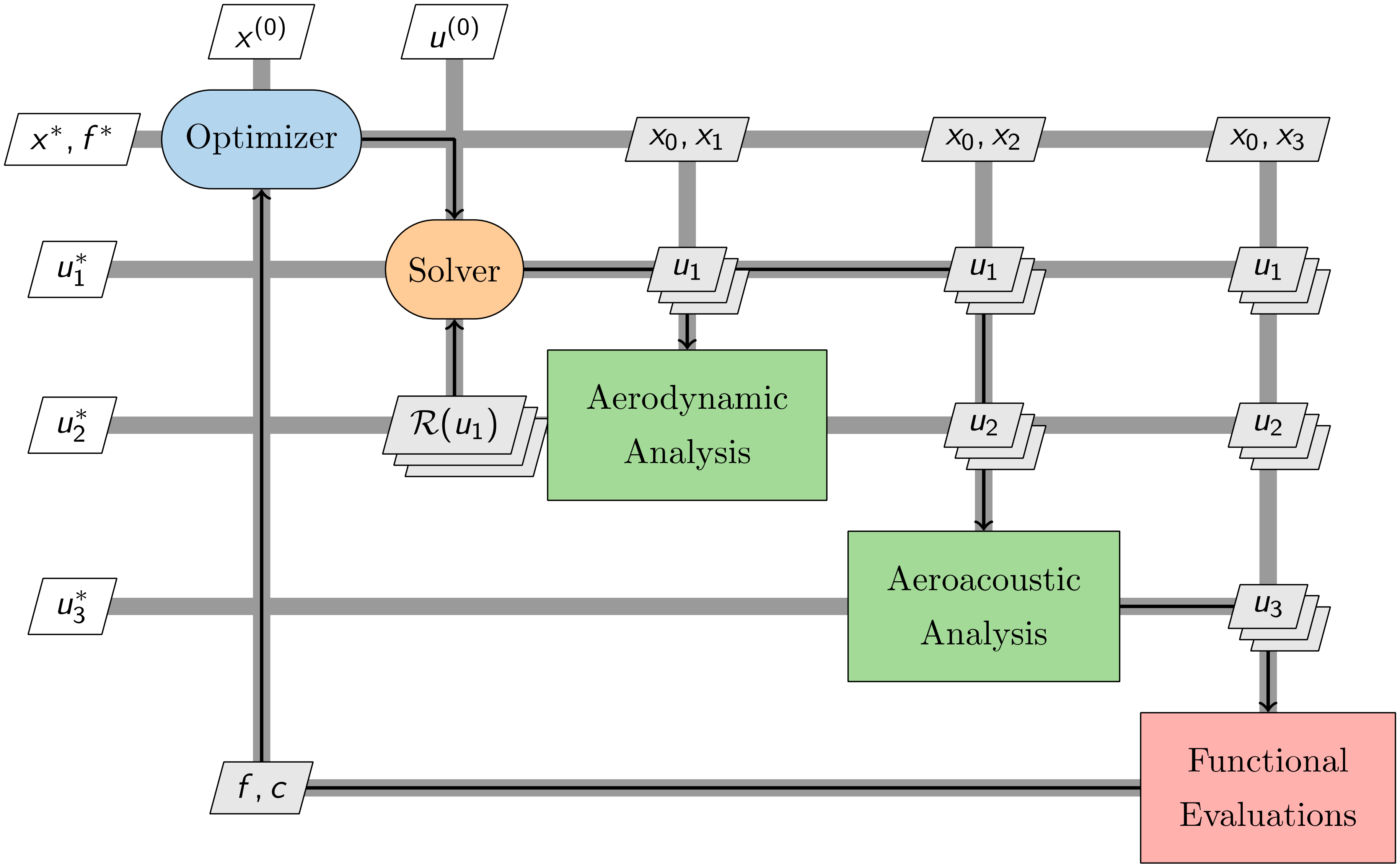

How can we predict UAM vehicle noise?

How can we characterize rotor noise?

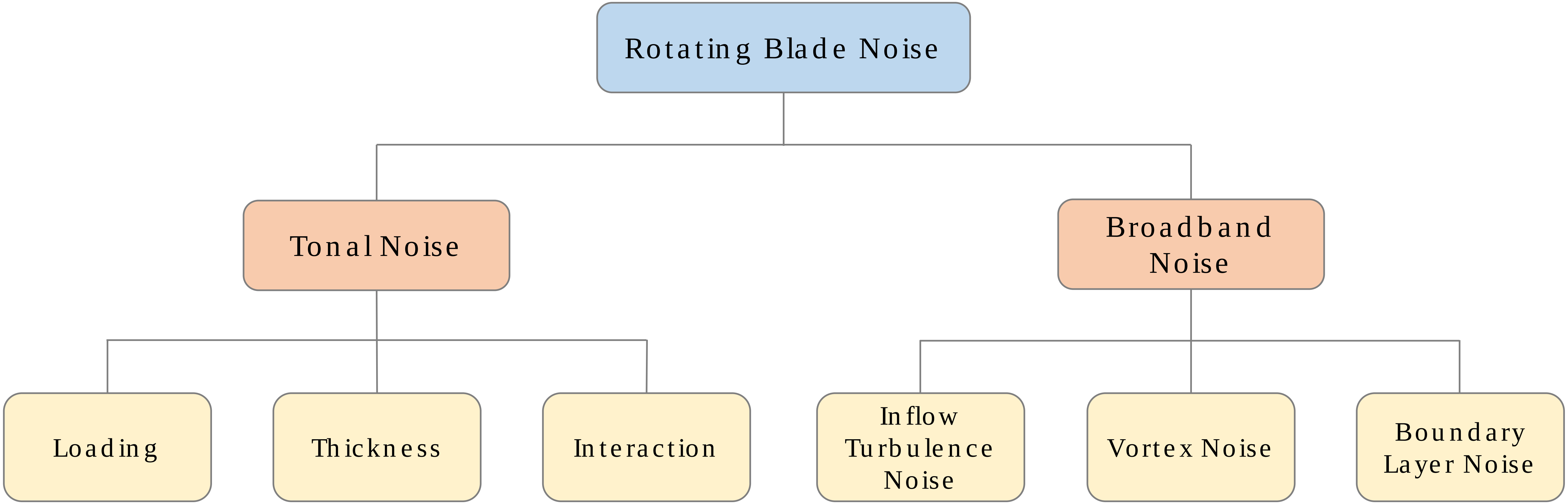

R J Pegg. A Summary and Evaluation of Semi-Empirical Methods for the Prediction of Helicopter Rotor Noise. Technical report, NASA Langley Research Center, 1979.

Tonal Noise Sources

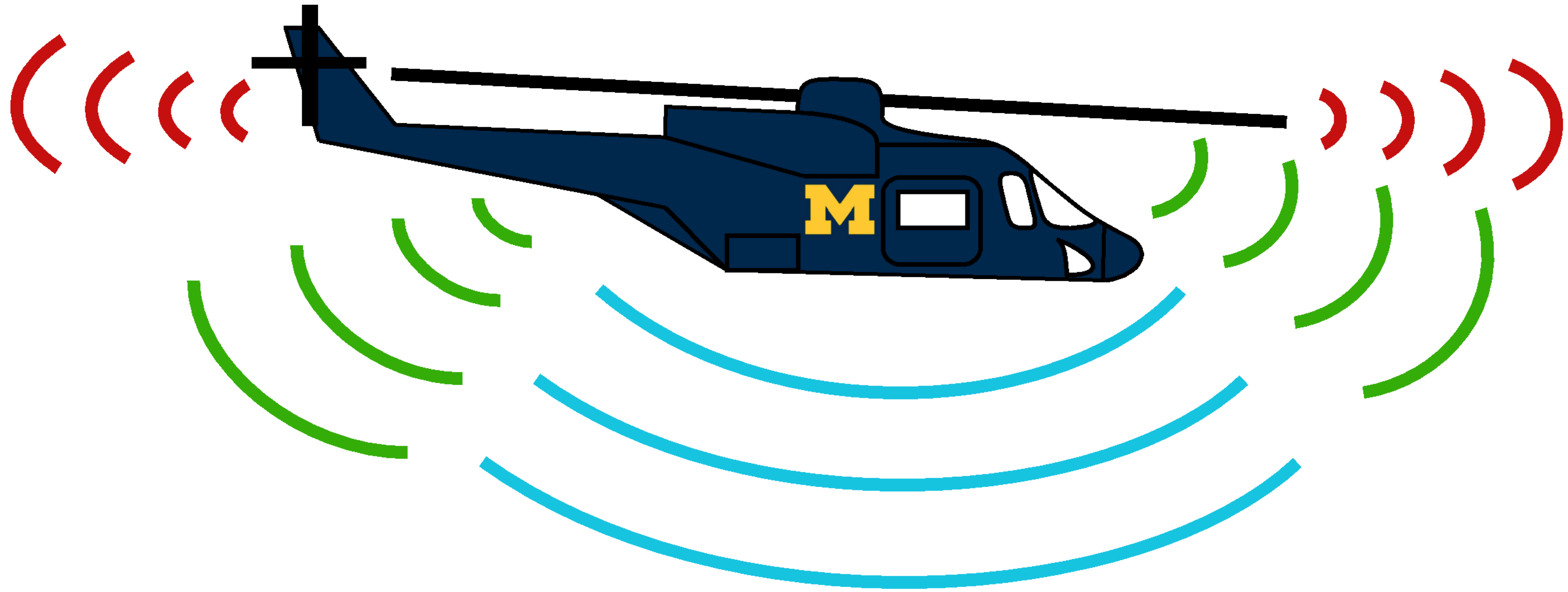

Kenneth S Brentner. Rotor Noise Modeling. Technical report, 5th Transformative Vertical Flight Workshop, San Francisco, California, 2018.

Broadband Noise Sources

Pegg Model

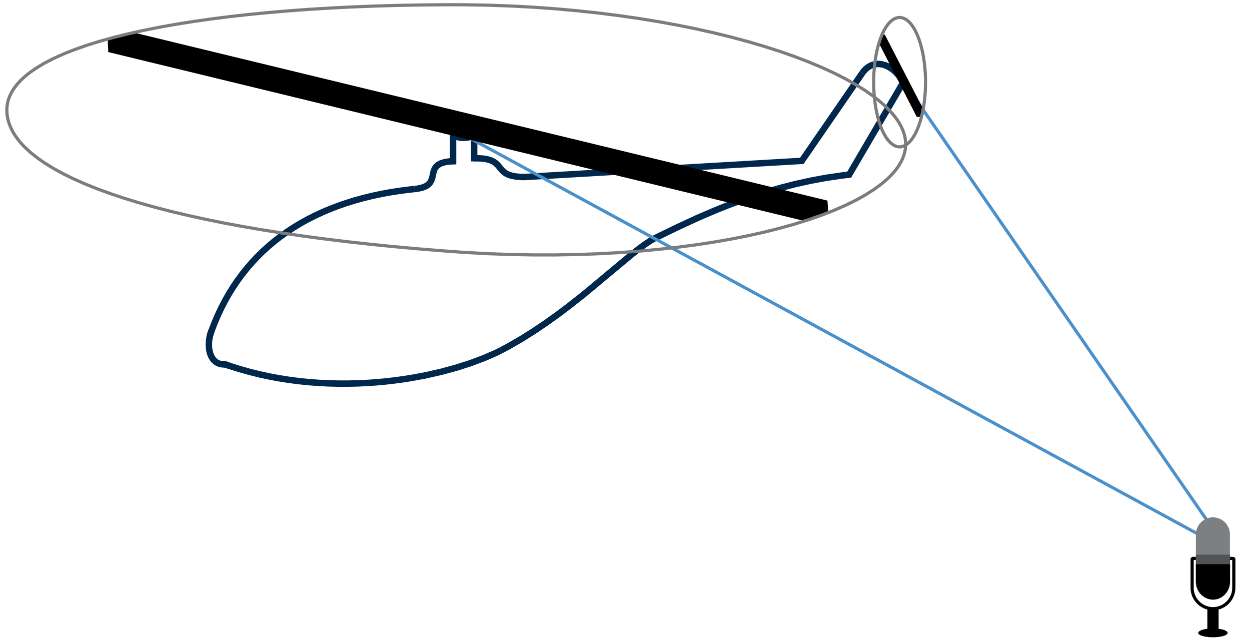

R J Pegg. A Summary and Evaluation of Semi-Empirical Methods for the Prediction of Helicopter Rotor Noise. Technical report, NASA Langley Research Center, 1979.

Brooks Model

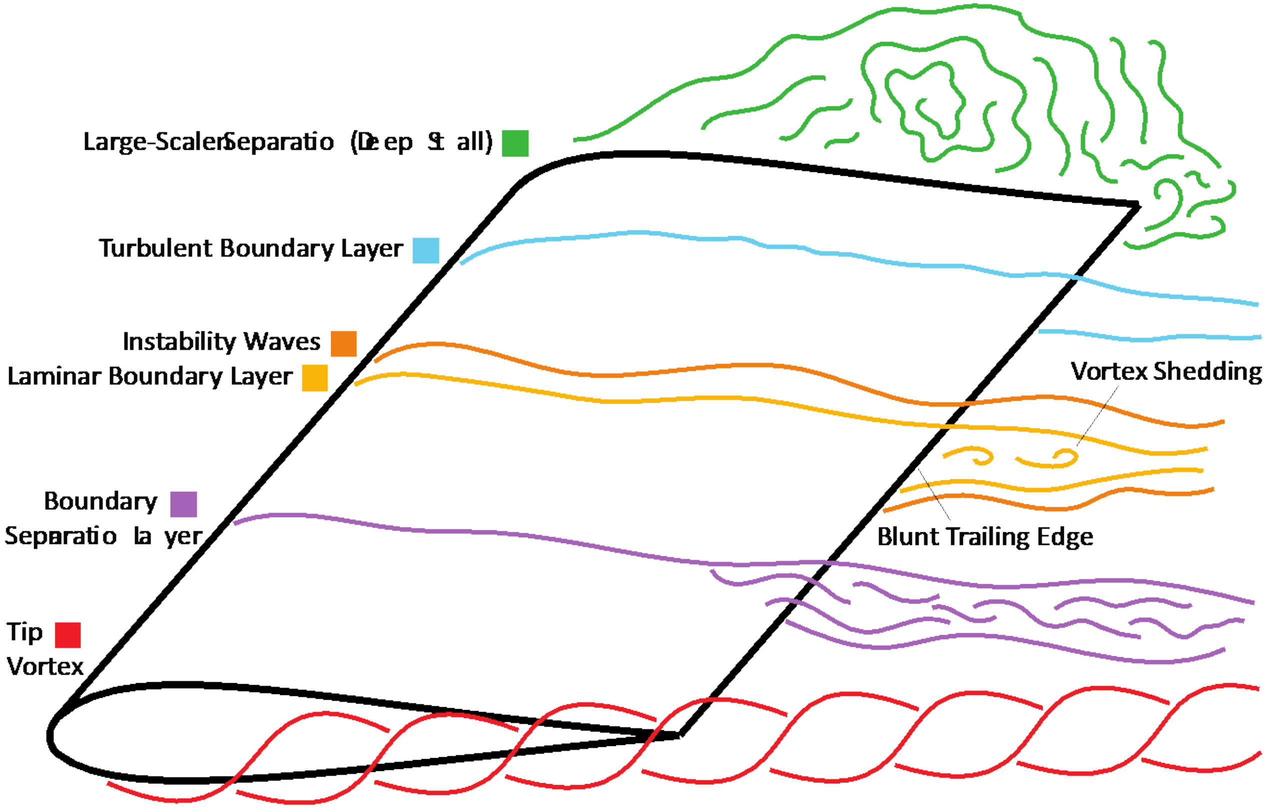

T F Brooks, S D Pope, and M A Marcolini. NASA Reference Publication 1218 Airfoil Self-Noise and Prediction. Technical report, NASA, Hampton, Virginia, 1989.

We are in the process of implementing a broadband noise model into our toolkit

Computational Aeroacoustics

- Techniques for aeroacoustic analysis:

1. Direct Numerical Simulation from Navier-Stokes Equation

2. Integral-Based Formulations

   i. Lighthill's Analogy
      - Exact rearrangement of the Navier-Stokes equation

   ii. Kirchhoff Method
      - Simplified acoustic source enclosed by a source-surface

   iii. Ffowcs Williams and Hawkings Model (FWH)
      - Based on Navier-Stokes equation with Lighthill's analogy with surface integrals over monopole, dipole, and quadrupole noise sources

Computationally Prohibitive for Multidisciplinary Design Optimization

Inaccurate for rotorcraft applications

Used (and validated) extensively for rotorcraft applications

Kenneth S. Brentner. Modeling aerodynamically generated sound: Recent advances in rotor noise prediction. In 38th Aerospace Sciences Meeting and Exhibit, number January, pages 1–11, Reno, Nevada, 2000.1

Tonal Noise Modeling

Ffowcs Williams and Hawkings:

$$4\pi a_0^2 \rho' = \underbrace{\cancel{\frac{\partial^2}{\partial x_i \partial x_j}\int_V \frac{HT_{ij}}{r\|1 - M_r\|} d^3\eta}}_{\text{Quadrupole}} - \underbrace{\frac{\partial}{\partial x_i}\int_S \frac{P_{ij} + \rho v_i(v_j - u_j)}{r\|1 - M_r\|} n_j dS(\eta)}_{\text{Dipole}} + \underbrace{\frac{\partial}{\partial t}\int_S \frac{\rho_0 u_i + \rho(v_i - u_i)}{r\,\|1 - M_r\|} n_i dS(\eta)}_{\text{Monopole}}$$

Noise due to density fluctuations

Noise due to loading

Noise due to thickness

Farassat Formulation 1A:

$$p_L'(\vec{x}, t) = \frac{1}{4\pi a_0}\int_S \left[\frac{\dot{L}_i \hat{r}_i}{r(1 - M_r)^2}\right]\Bigg|_{\tau^*} dS + \frac{1}{4\pi}\int_S \left[\frac{L_i(\hat{r}_i - M_i)}{r^2(1 - M_r)^2}\right]\Bigg|_{\tau^*} dS + \frac{1}{4\pi a_0}\int_S \left[\frac{L_i \hat{r}_i\left(r\dot{M}_i \hat{r}_i + a_0(M_i\,\hat{r}_i - M_i M_i)\right)}{r^2(1 - M_r)^3}\right]\Bigg|_{\tau^*} dS$$

$$p_T'(\vec{x}, t) = \frac{1}{4\pi}\int_S \left[\frac{\rho_0 \dot{u}_n}{r(1 - M_r)^2}\right]\Bigg|_{\tau^*} dS + \frac{1}{4\pi}\int_S \left[\frac{\rho u_n\left(r\dot{M}\hat{r}_i + a_0(M_i\,\hat{r}_i - M_i M_i)\right)}{r^2(1 - M_r)^3}\right]\Bigg|_{\tau^*} dS$$

* This work uses a compact model for monopole noise, as opposed to the monopole component of Farassat Formulation 1A

Noise Metric: Sound Pressure Level [dB]:

$$SPL = 10 \cdot \log_{10}\left(\left[\frac{p'_{rms}}{p_{ref}}\right]^2\right)$$

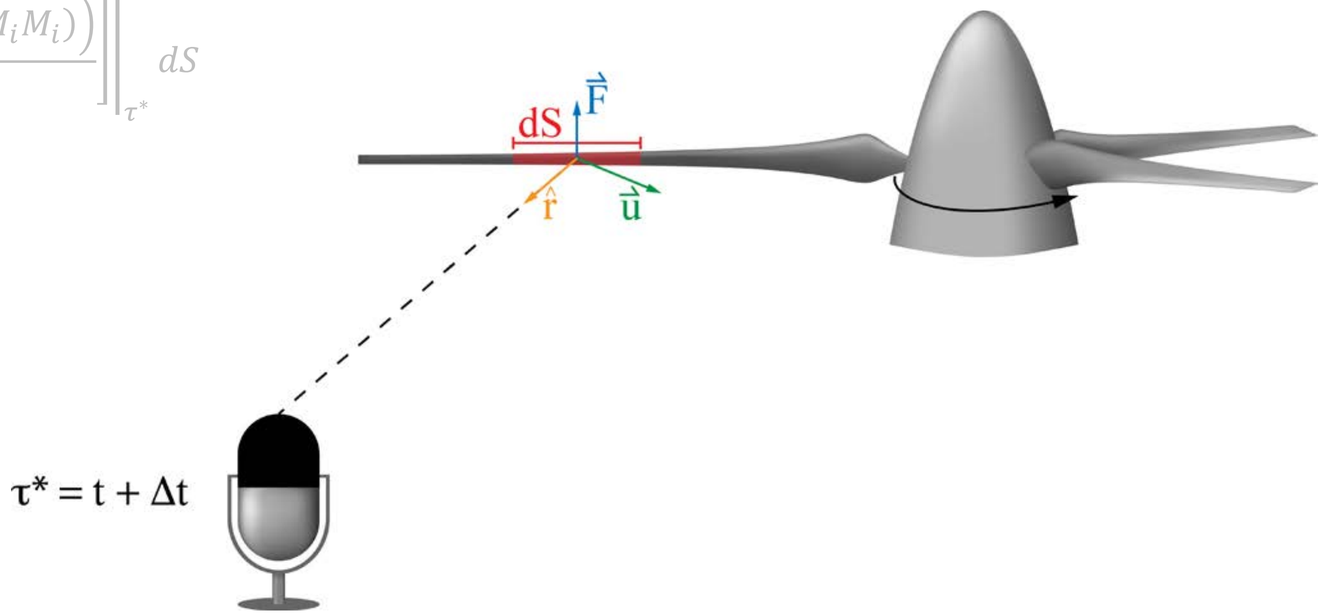

J E Ffowcs Williams and D L Hawkings. Sound Generation by Turbulence and Surfaces in Arbitrary Motion. Technical Report 1151, Royal Society, 1969.

Noise Modeling is a Time-Accurate Problem

- Evaluate the pressure perturbation due to the rotor at each observer point of interest

- Compute the total sound pressure level based on the time-history of the pressure perturbation at each observer point

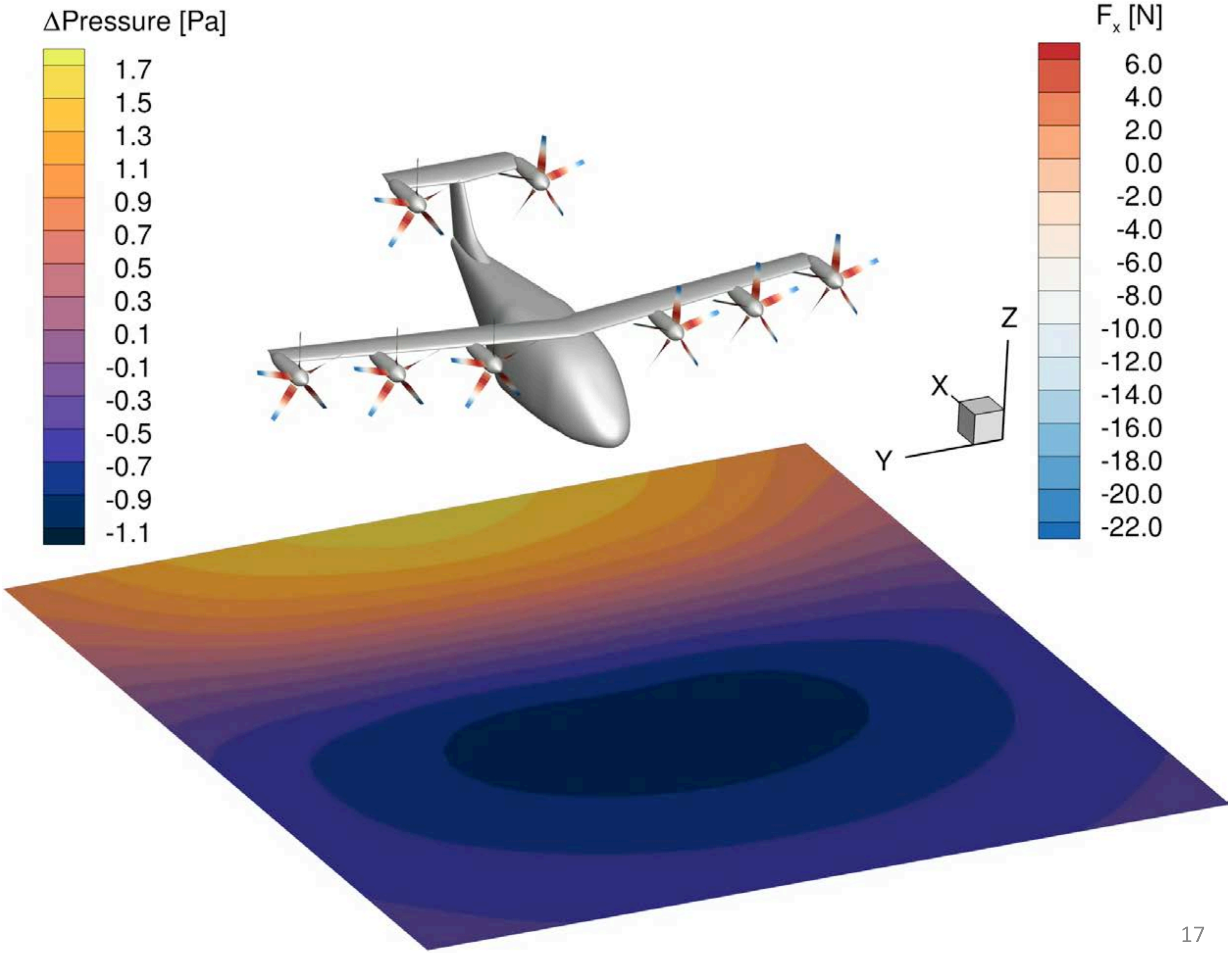

Aerodynamic Modeling

Hybrid Blade Element Momentum Theory (HBEM)

Momentum Theory

- Models a rotor as a disk, operating within a stream tube

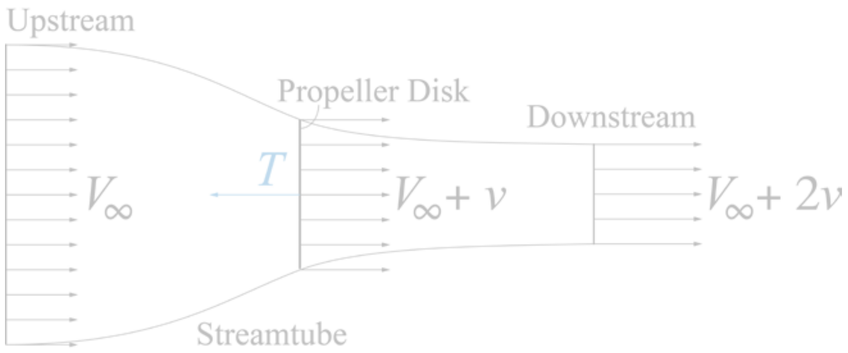

Coefficient of Thrust:

$$C_{T,MT} = \frac{T_{des}}{\pi \rho V_t^2 R^2}$$

Blade Element Theory

- Considers blade section data to compute aerodynamic loads along rotor blade span

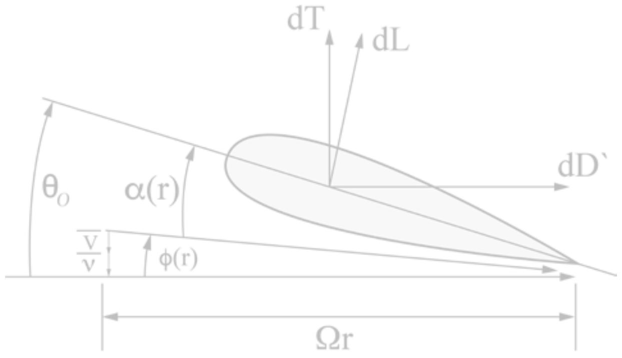

Coefficient of Thrust:

$$C_{T,BET} = \frac{N_b}{4R^2\pi^2} \int_0^R \int_0^{2\pi} C_l u^2 c(r) \cos(\phi) \, d\phi \, dr$$

$$\mathcal{R}(T_{\text{mag}}) = C_{T,BET}(T_{\text{mag}}) - C_{T,MT}(T_{\text{mag}}) \Rightarrow 0$$

➞ This analysis is quasi-steady, making it more efficient and easier to manage than fully unsteady methods

Computing Derivatives

Implicit Derivatives:

$\boldsymbol{x}$: Design Variables
$\boldsymbol{u}$: State Variables

$f = f(\boldsymbol{x}, \boldsymbol{u}(\boldsymbol{x}))$: Function of Interest

$\mathcal{R}(\boldsymbol{x}, \boldsymbol{u}(\boldsymbol{x})) = 0$: Solution Residual

$$\underbrace{\frac{df}{d\boldsymbol{x}}}_{n_f \text{ x } n_x} = \underbrace{\frac{\partial f}{\partial \boldsymbol{x}}}_{n_f \text{ x } n_x} + \underbrace{\frac{\partial f}{\partial \boldsymbol{u}}}_{n_f \text{ x } n_u} \underbrace{\frac{d\boldsymbol{u}}{d\boldsymbol{x}}}_{n_u \text{ x } n_x}$$

$$\underbrace{\frac{d\mathcal{R}}{d\boldsymbol{x}}}_{n_\mathcal{R} \text{ x } n_x} = \underbrace{\frac{\partial \mathcal{R}}{\partial \boldsymbol{x}}}_{n_\mathcal{R} \text{ x } n_x} + \underbrace{\frac{\partial \mathcal{R}}{\partial \boldsymbol{u}}}_{n_\mathcal{R} \text{ x } n_u} \underbrace{\frac{d\boldsymbol{u}}{d\boldsymbol{x}}}_{n_u \text{ x } n_x} = 0$$

$$\Rightarrow \frac{d\boldsymbol{u}}{d\boldsymbol{x}} = -\left[\frac{\partial \mathcal{R}}{\partial \boldsymbol{u}}\right]^{-1} \frac{\partial \mathcal{R}}{\partial \boldsymbol{x}}$$

Dimensions:
- Design Variables: $n_x = \mathcal{O}(10)$
- State Variables: $n_u = \mathcal{O}(100)$
- Functions of Interest: $n_f = \mathcal{O}(1)$
- Residual Values: $n_\mathcal{R} = \mathcal{O}(100)$

$$\frac{df}{d\boldsymbol{x}} = \frac{\partial f}{\partial \boldsymbol{x}} - \underbrace{\frac{\partial f}{\partial \boldsymbol{u}}\left[\frac{\partial \mathcal{R}}{\partial \boldsymbol{u}}\right]^{-1}}_{\psi^T} \overbrace{\left[\frac{\partial \mathcal{R}}{\partial \boldsymbol{u}}\right]^{-1}\frac{\partial \mathcal{R}}{\partial \boldsymbol{x}}}^{\phi}$$

$$\underbrace{\frac{\partial \mathcal{R}}{\partial \boldsymbol{u}}}_{n_\mathcal{R} \text{ x } n_u} \underbrace{\phi}_{n_u \text{ x } n_x} = \underbrace{\frac{\partial \mathcal{R}}{\partial \boldsymbol{x}}}_{n_\mathcal{R} \text{ x } n_x}$$: Direct Method

$$\underbrace{\left[\frac{\partial \mathcal{R}}{\partial \boldsymbol{u}}\right]^T}_{n_u \text{ x } n_\mathcal{R}} \underbrace{\psi}_{n_u \text{ x } 1} = \underbrace{\left[\frac{\partial f}{\partial \boldsymbol{u}}\right]^T}_{n_u \text{ x } 1}$$: Adjoint Method

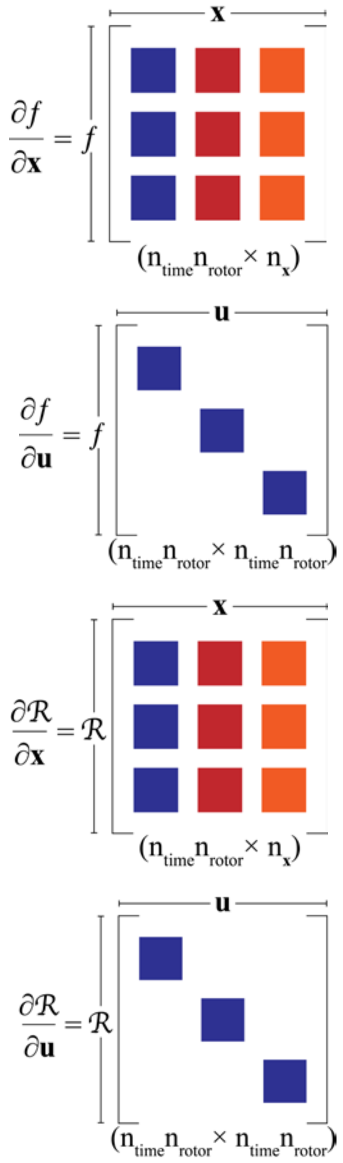

→ Derivatives computed using algorithmic differentiation, leveraging graph coloring

Coupled Aerodynamic and Aeroacoustic Optimization

- Aerodynamic and aeroacoustic analysis tools wrapped with OpenMDAO for model coupling

- Derivatives computed and passed between models internally within OpenMDAO

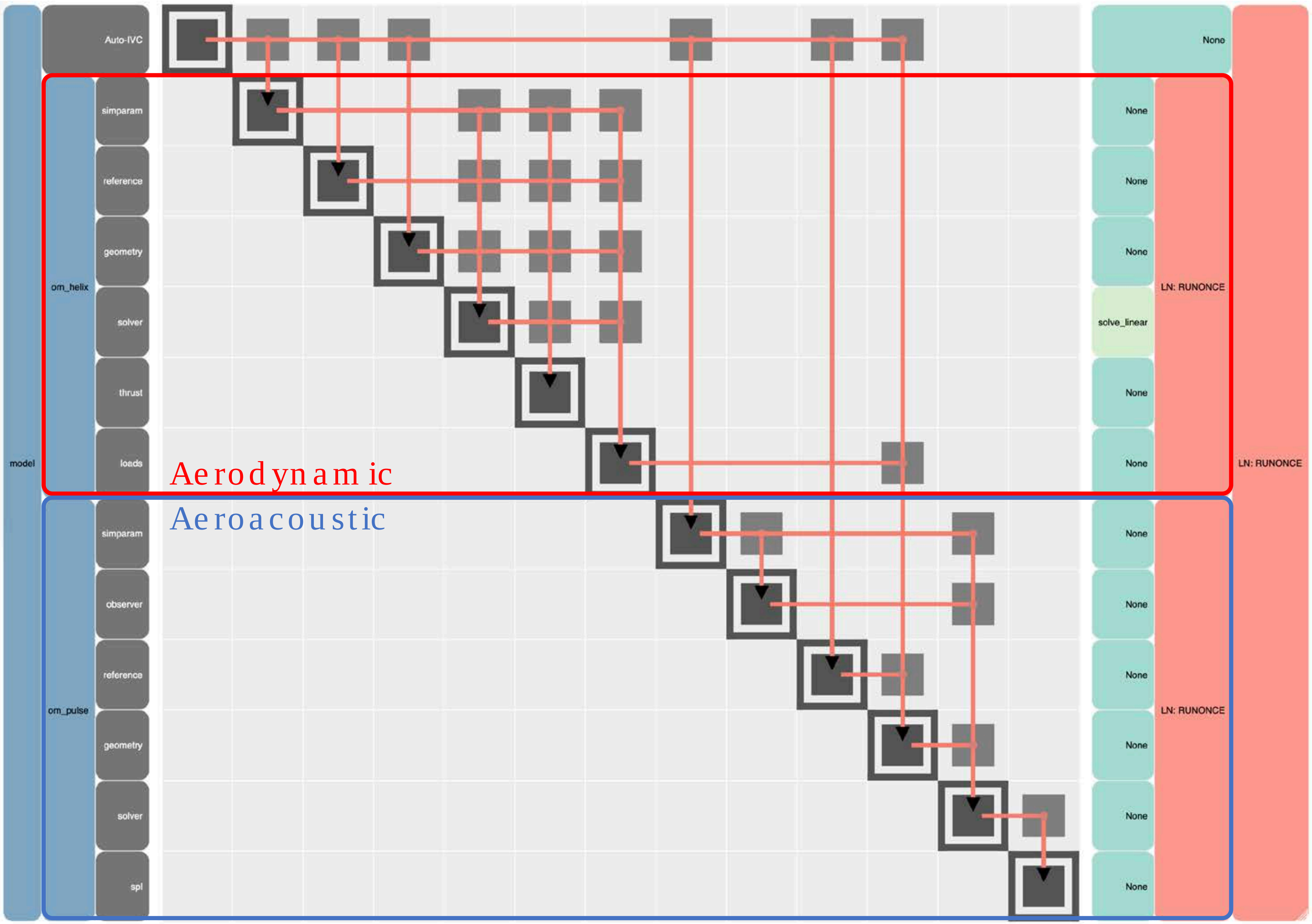

How does this workflow perform?

Example Optimization Problem: NASA N+1 UAM Quadrotor Concept Vehicle

- Single-passenger
- Fully electric
- RPM control

Johnson, W., & Silva, C. (2022). NASA concept vehicles and the engineering of advanced air mobility aircraft. *The Aeronautical Journal, 126*(1295), 59-91. doi:10.1017/aer.2021.92

Quadrotor Optimization: Baseline Analysis

- Performed simulations and optimizations at three spanwise design variable resolutions: 5, 10, 15 variables.
- Blade loads and SPL for 15 spanwise variable analyses:

Maximum SPL [dB]	Thrust [N]
80.464555	1438.324294

Blade Loads

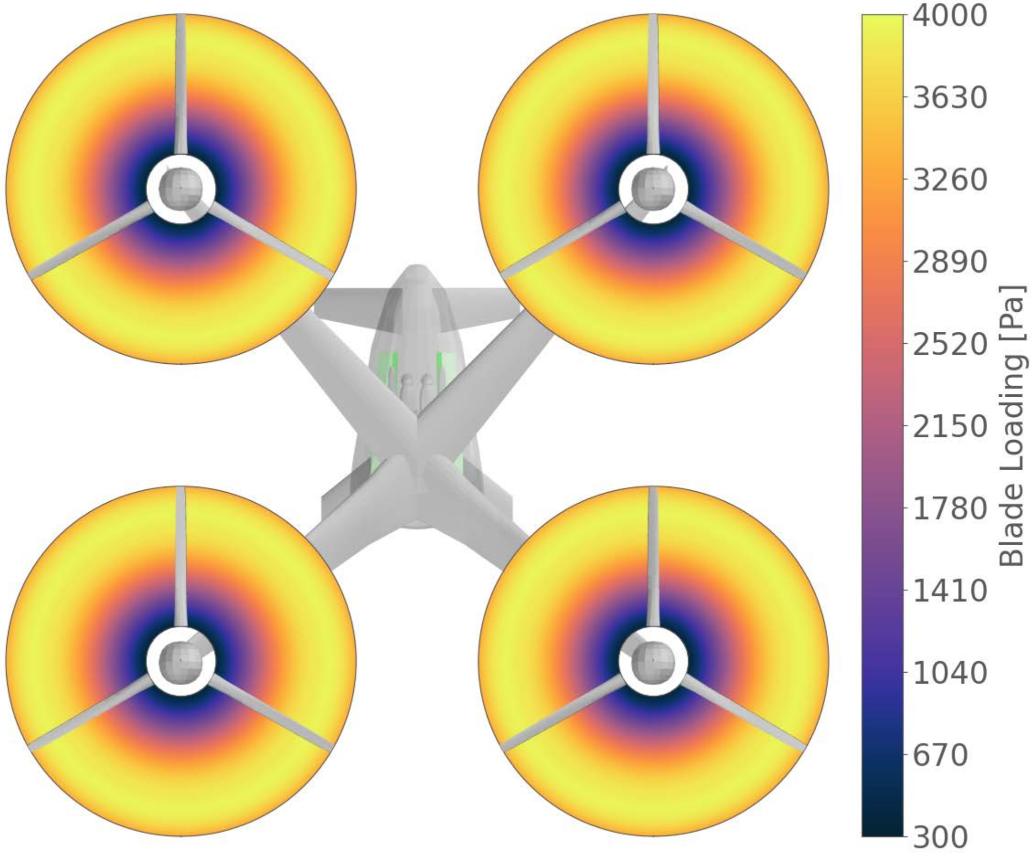

Sound Pressure Level

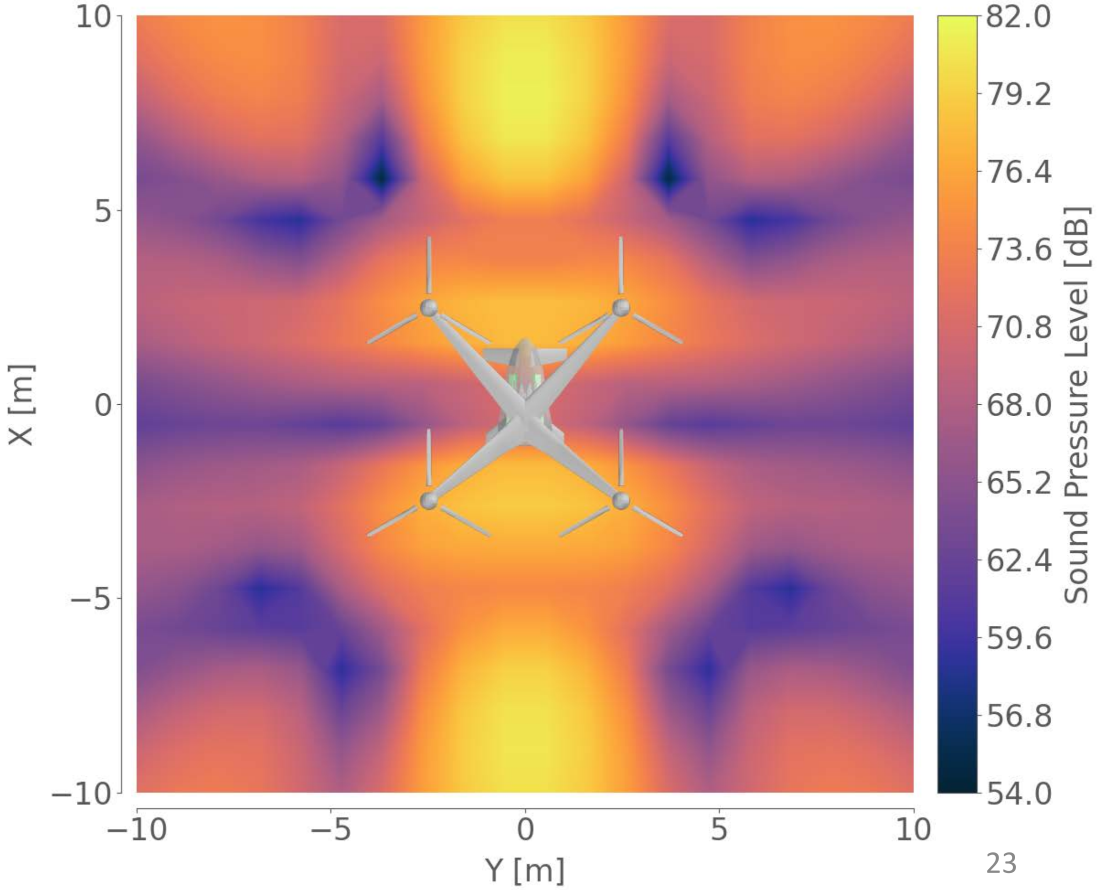

Johnson, W., Silva, C., and Solis, E., "Concept Vehicles for VTOL Air Taxi Operations," Aeromechanics Design for Transformative Vertical Flight, San Francisco, California, 2018, pp. 1–24

Quadrotor Optimization: Result

Optimization Problem Statement:

	Function or Variable	Units	Description	Quantity
Minimize	KS(SPL)	dB	KS aggregated sound pressure level	1
With respect to	Twist	°	Blade twist distribution	5/10/15
	Chord	m	Blade chord distribution	5/10/15
	ω	rad/s	Rotor rotation rate	1
			Total design variables	11/21/31
Subject to	$Thrust_z = 1429.175345$	N	Single rotor thrust required for ¼ vehicle weight	1
			Total constraints	1

Optimization Results:

SPL [dB]	73.856633
$Thrust_z$ [N]	1429.174531
ω [rad/s]	61.128316

Spanwise Distribution:

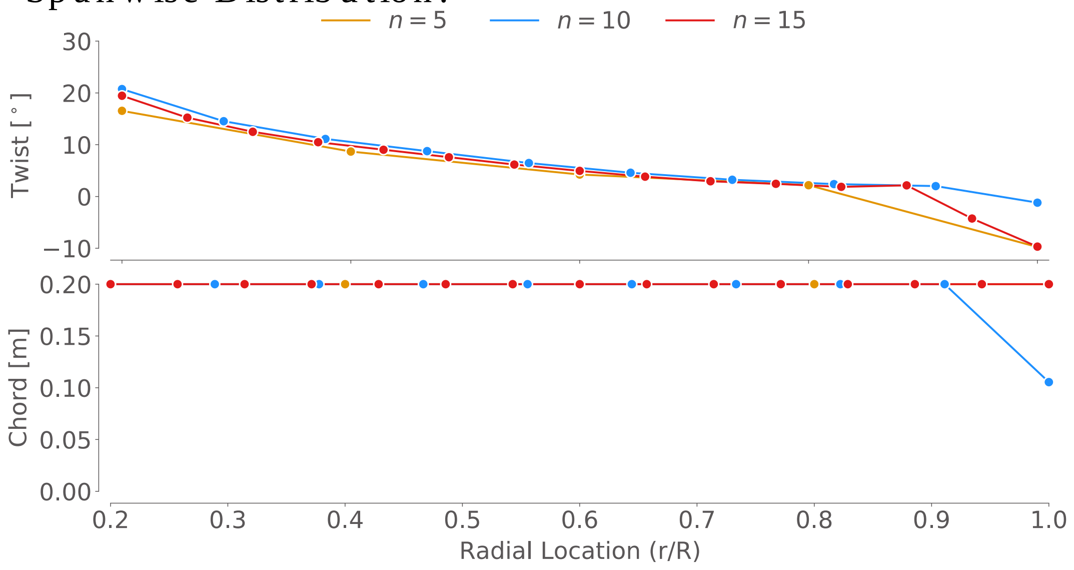

7dB reduction in noise

Blade Loading

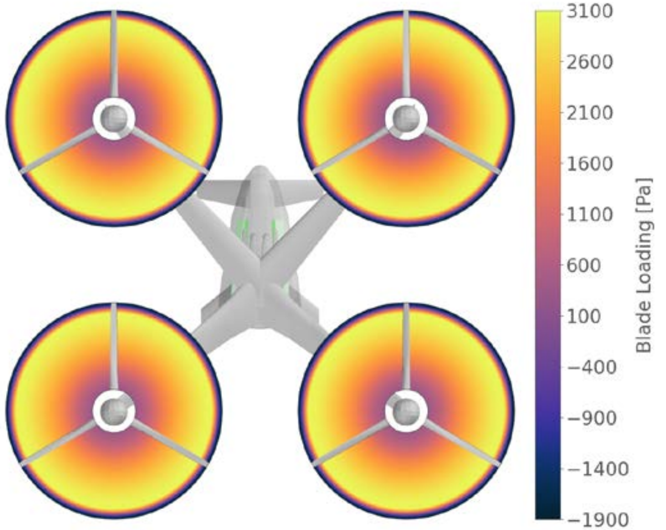

Sound Pressure Level

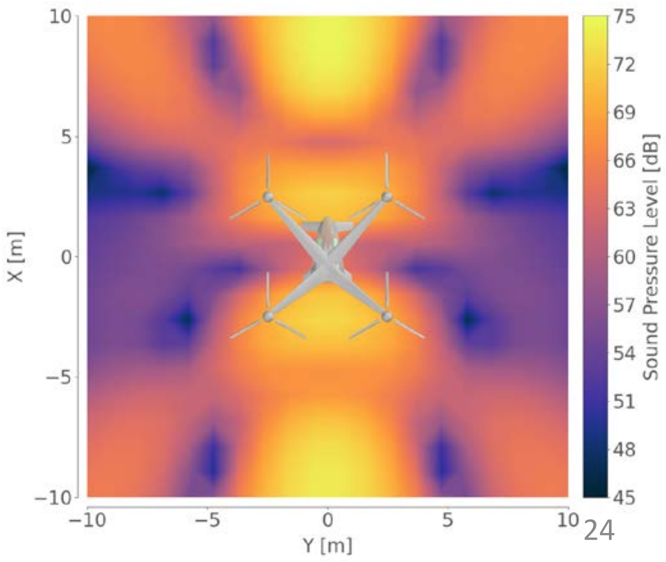

How can we implement this for aero-structural-acoustic optimization?

Aero-structural-acoustic Optimization

- Mixed-fidelity analysis to combine time-accurate and steady-state analyses within a single optimization

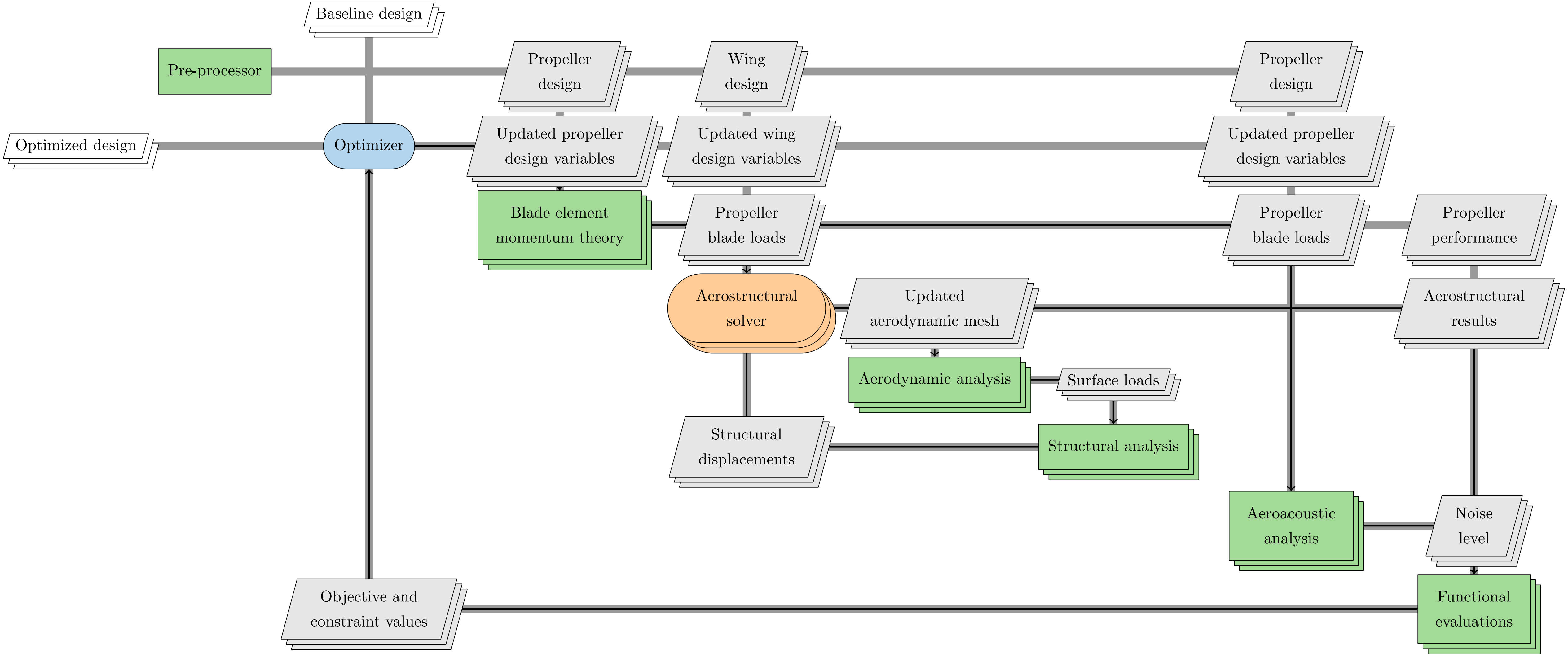

→ Built into the MPhys framework

Aerodynamic Analysis

- Analyzing the NASA Tiltwing Concept vehicle performance using DAFoam and actuator disk theory

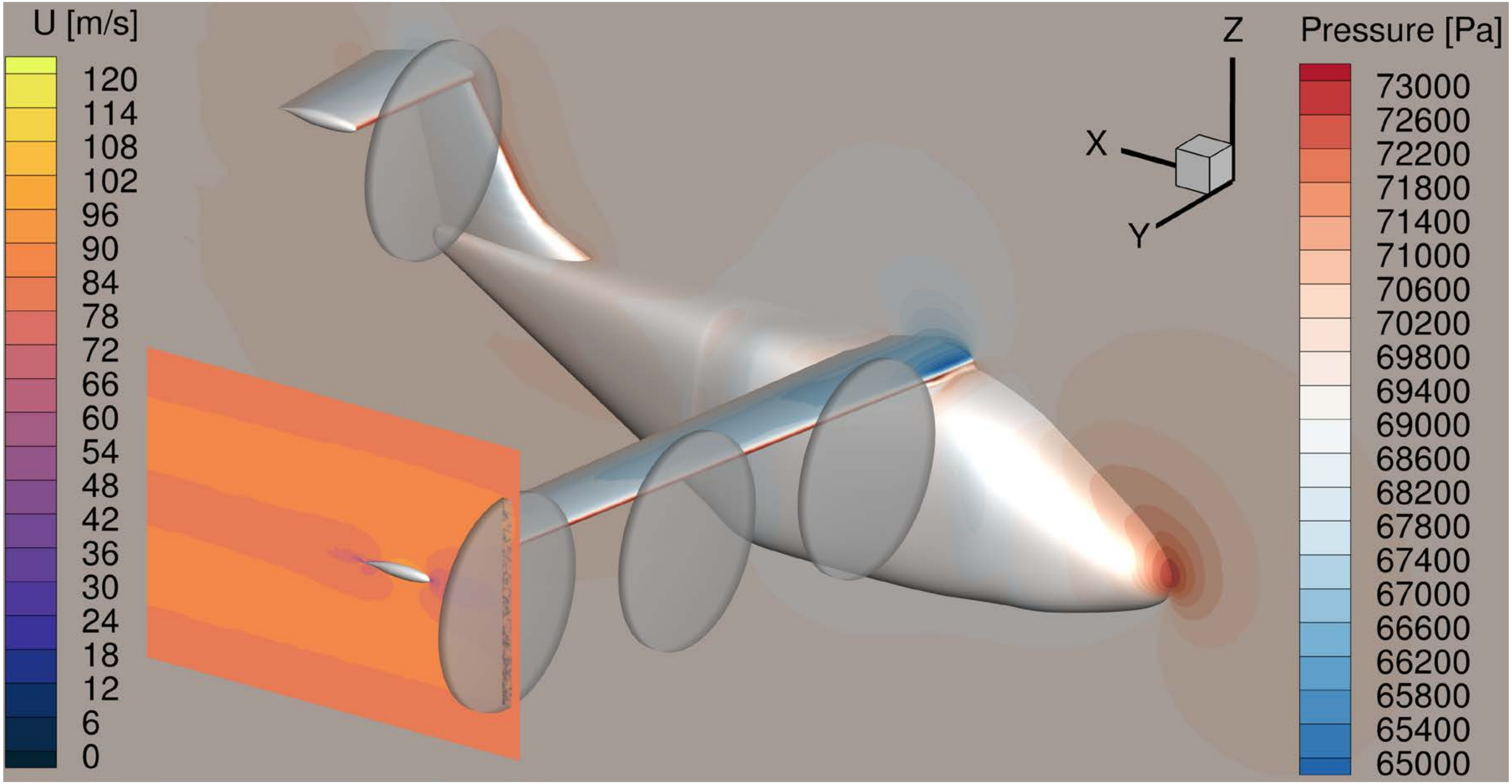

DAFoam + TACS: Aerostructural Optimization

- Adapted MPhys, DAFoam, and aerostructural coupling with FUNtoFEM and TACS to allow for propeller deflection under wing deformation

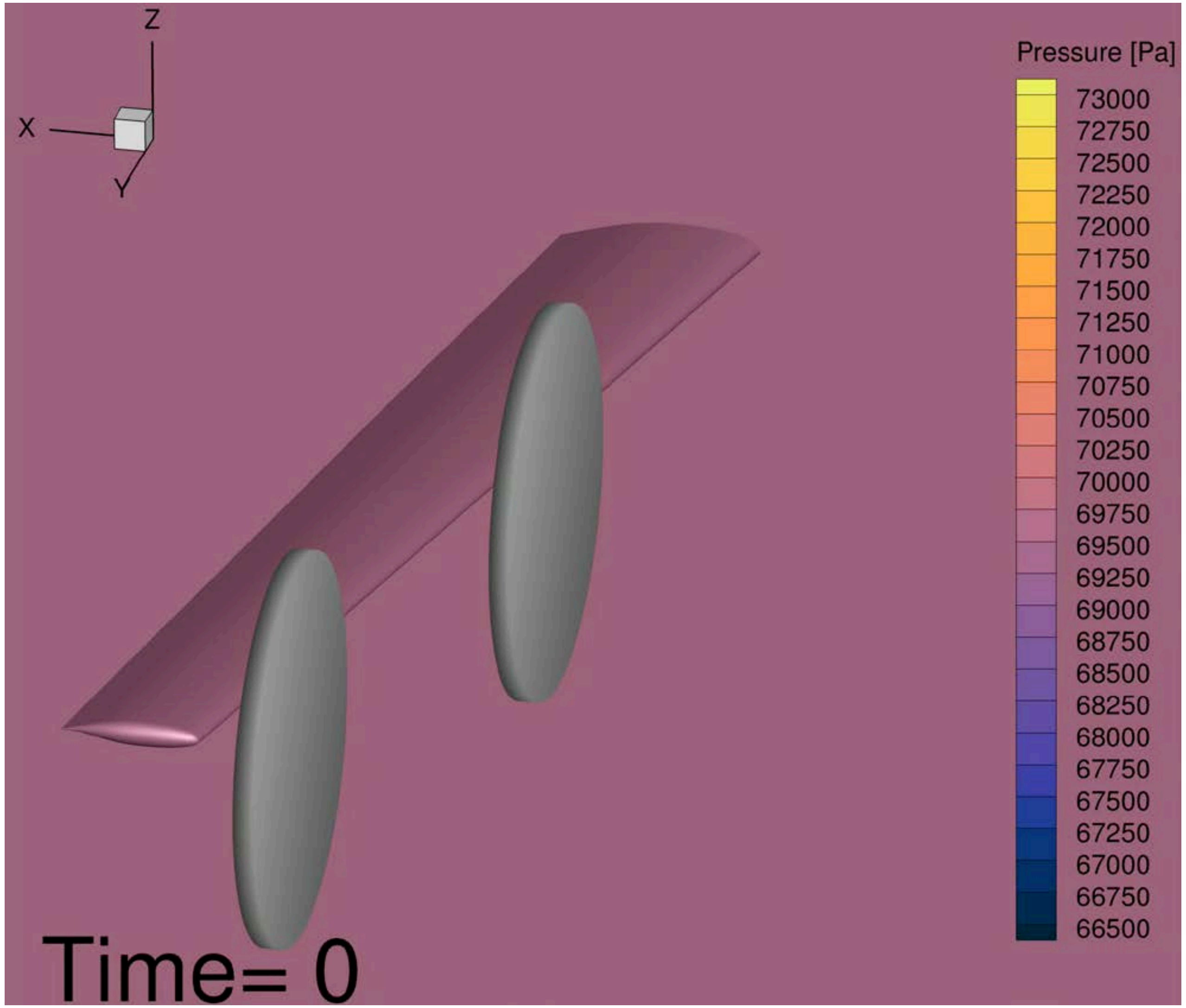

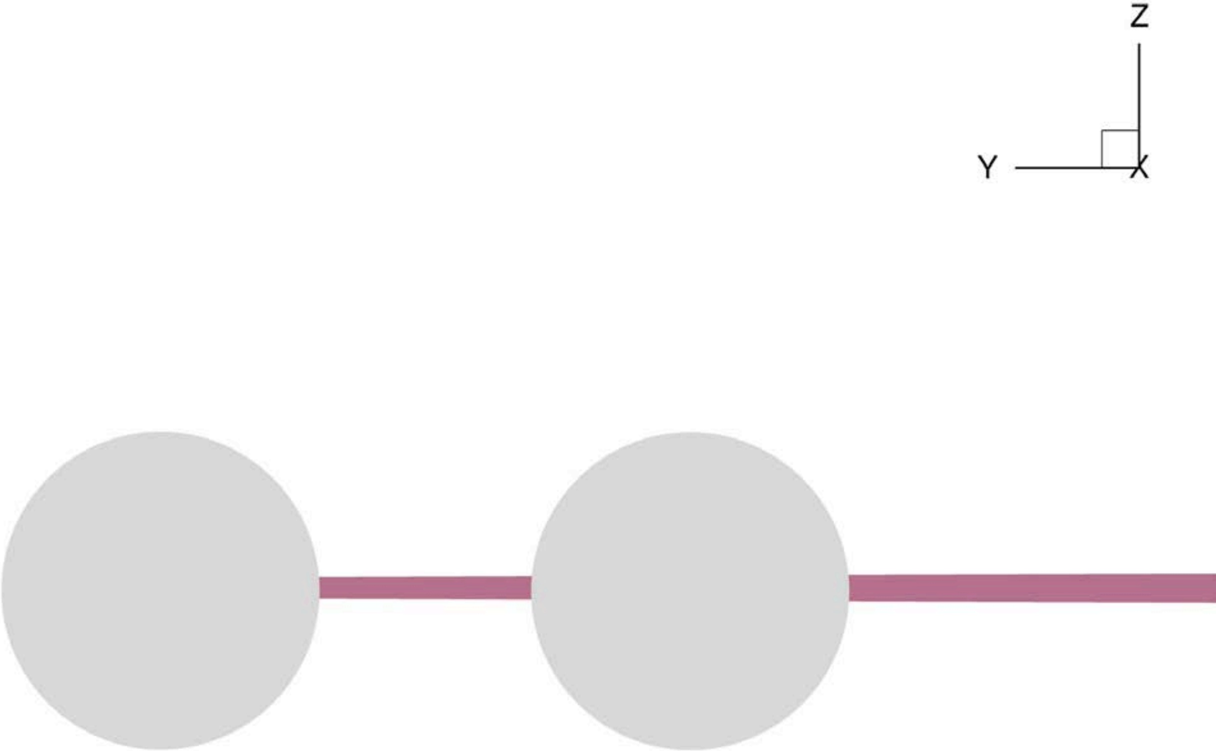

Conclusions and Next Steps

- Implemented a set of gradient-based optimization tools within OpenMDAO to work towards enabling aero-structural-acoustic optimization

- Working to implement our adjoint-based HBEM solver and aeroacoustic analysis tool into MPHYS

- Actively working towards aero-structural-acoustic optimization of a UAM tiltwing vehicle
  - We'll have more to say about this tomorrow during the MPhys workshop

- Broader methods development needed to move to higher fidelity aerodynamic analysis
  - How do we implement a coupled unsteady adjoint?

Thank you! Questions?

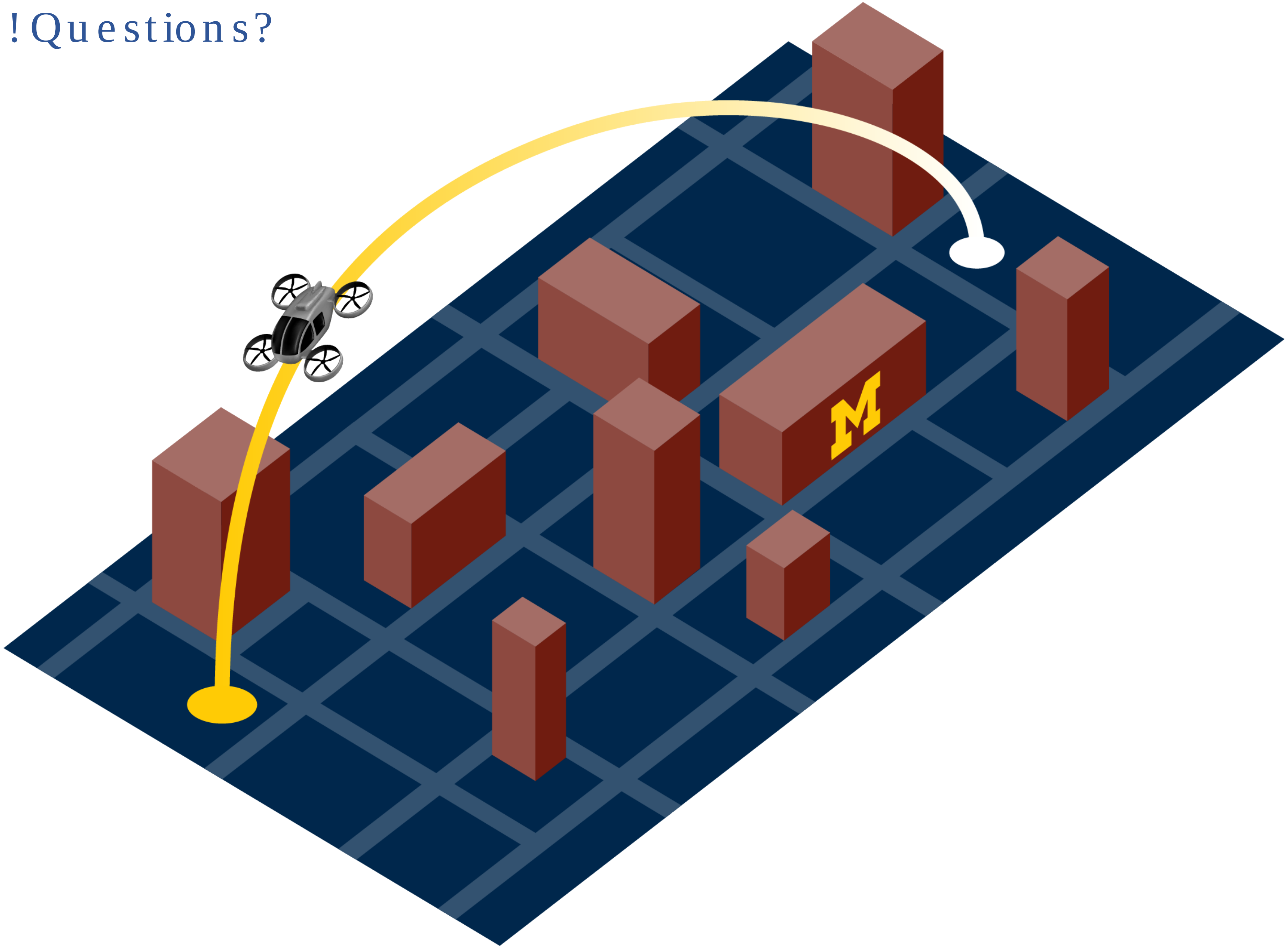

BACKUP

A^3 Vahana: Parametric Noise Study

https://www.airbus.com/newsroom/stories/vahana-marks-a-major-milestone-with-successful-full-transition-flight.html

Aerodynamic Analysis Tool

DUST Mid-Fidelity Aerodynamic Analysis Tool

- Relies on Helmholtz decomposition of velocity field
- Mixed boundary elements – vortex particle method and based on free vorticity evolution
- Allows for range of different fidelity aerodynamic models

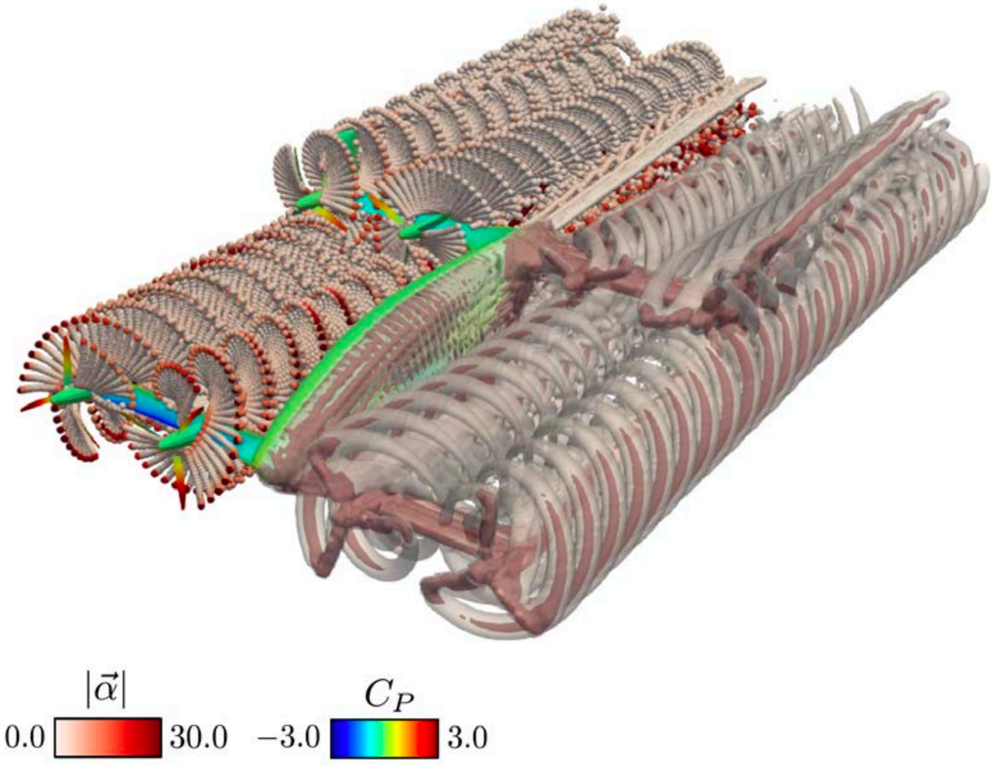

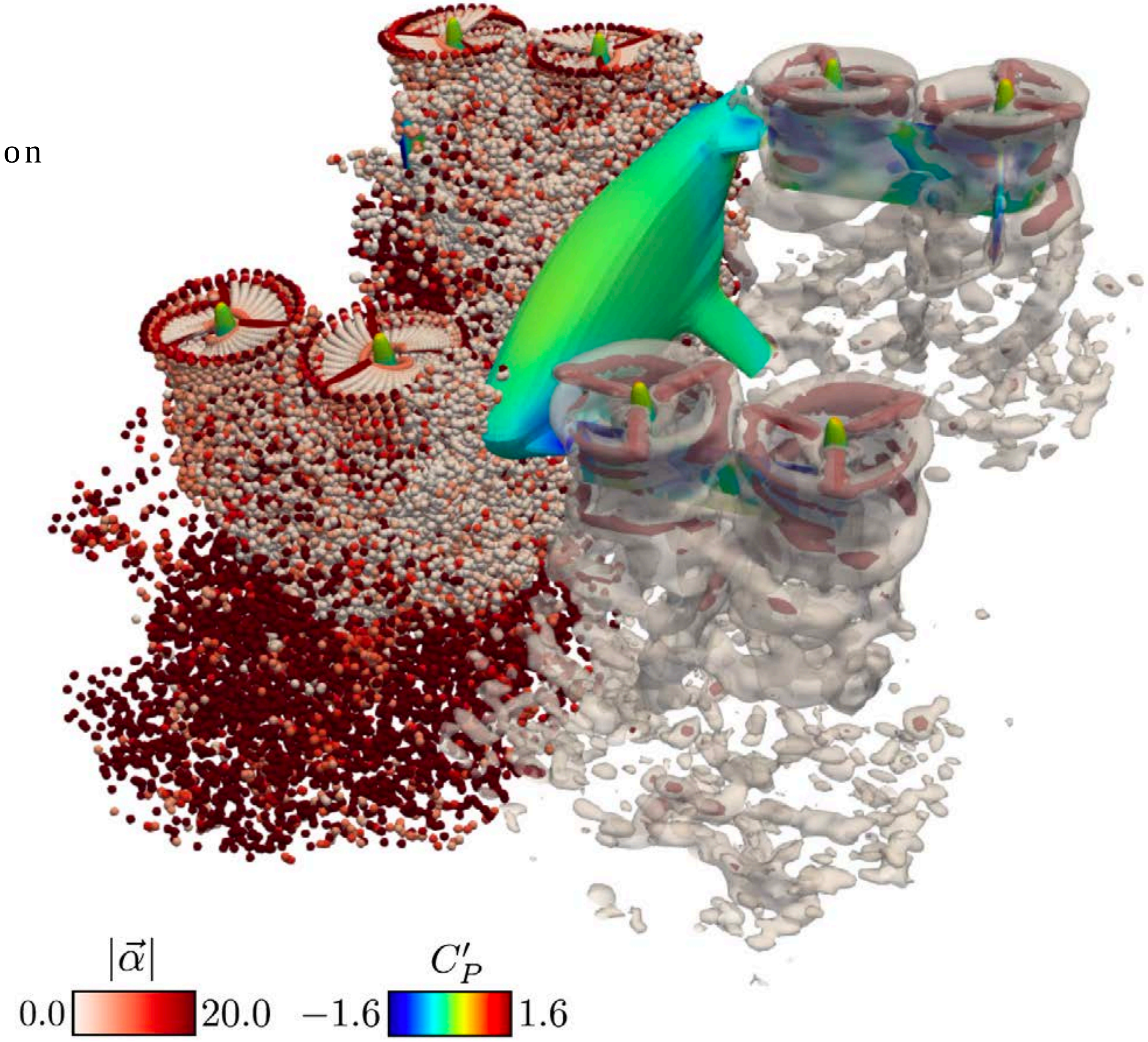

Reproduced with permission by the authors from: *D Montagnani, M Tugnoli, F Fonte, A Zanotti, M Syal, and G Droandi. Mid-Fidelity Analysis of Unsteady Interactional Aerodynamics of Complex Vtol Configurations. In 45th European Rotorcraft Forum, pages 1–11, Warsaw, Poland, 2019.*

Single Fan Aerodynamic Analysis

Particle evolution in hover flight condition

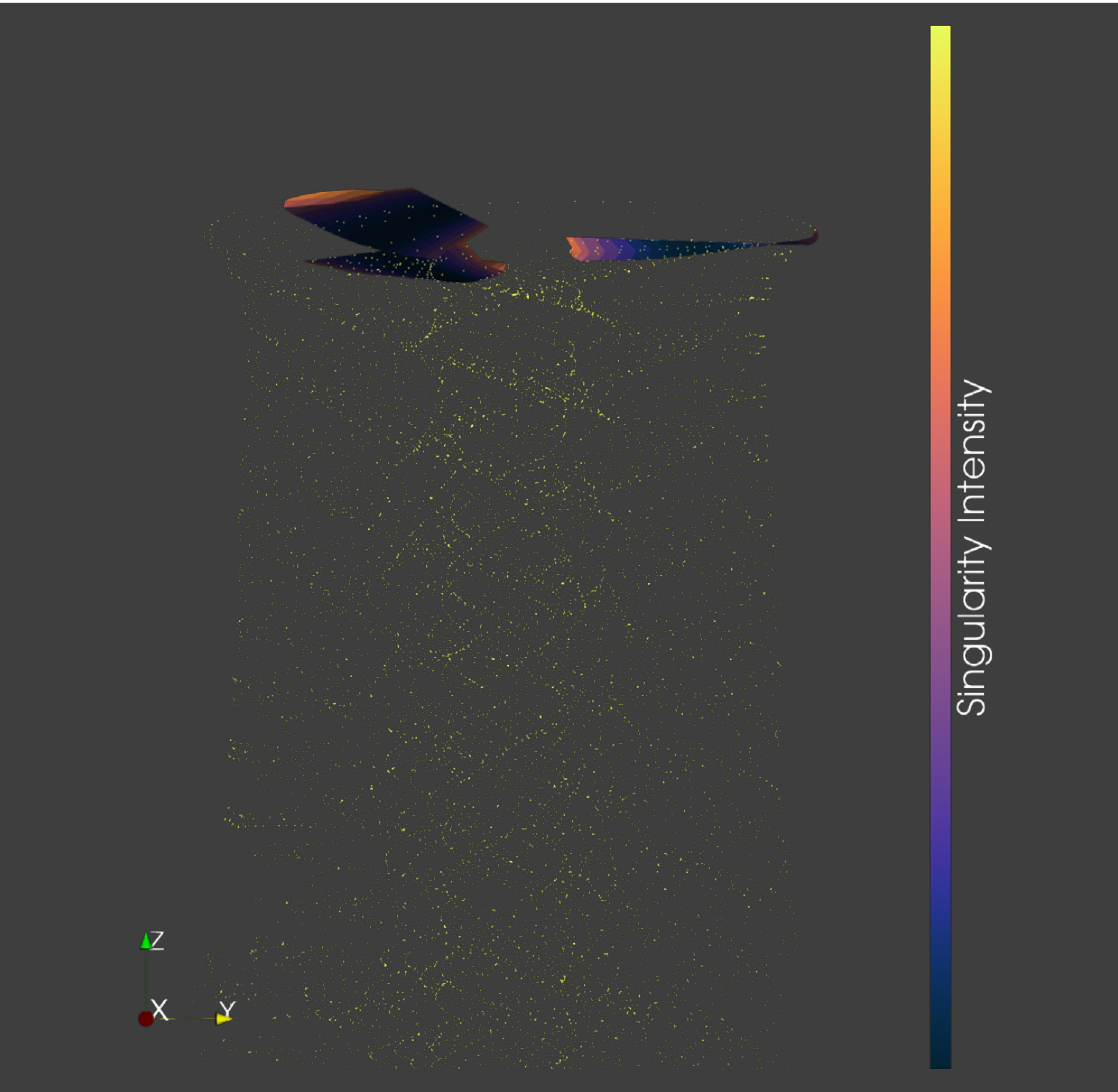

Cut plane of averaged velocity contours in hover flight

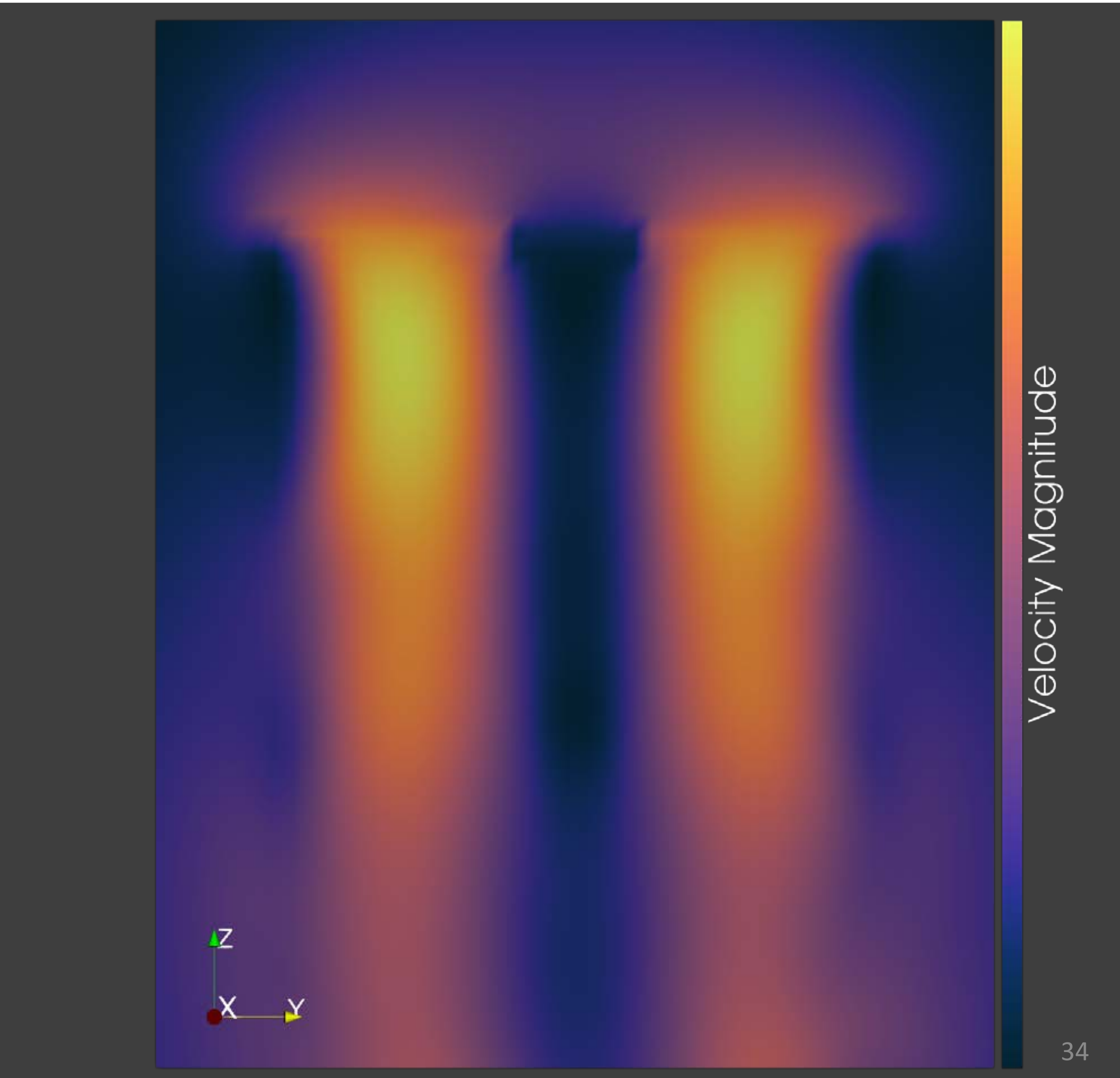

Single Fan Aeroacoustic Analysis

- Contour plots of Sound Pressure Level on planes below and in front of fan
    - Observer plane in front of fan:
        - [X,Y,Z] = [-250, 100, -250] - [250, 100, 250][m]
        - Grid of [50 x 50] observer probes
    - Observer plane below fan:
        - [X,Y,Z] = [-250, -250, -50] - [250, 250, -50][m]
        - Grid of [50 x 50] observer probes

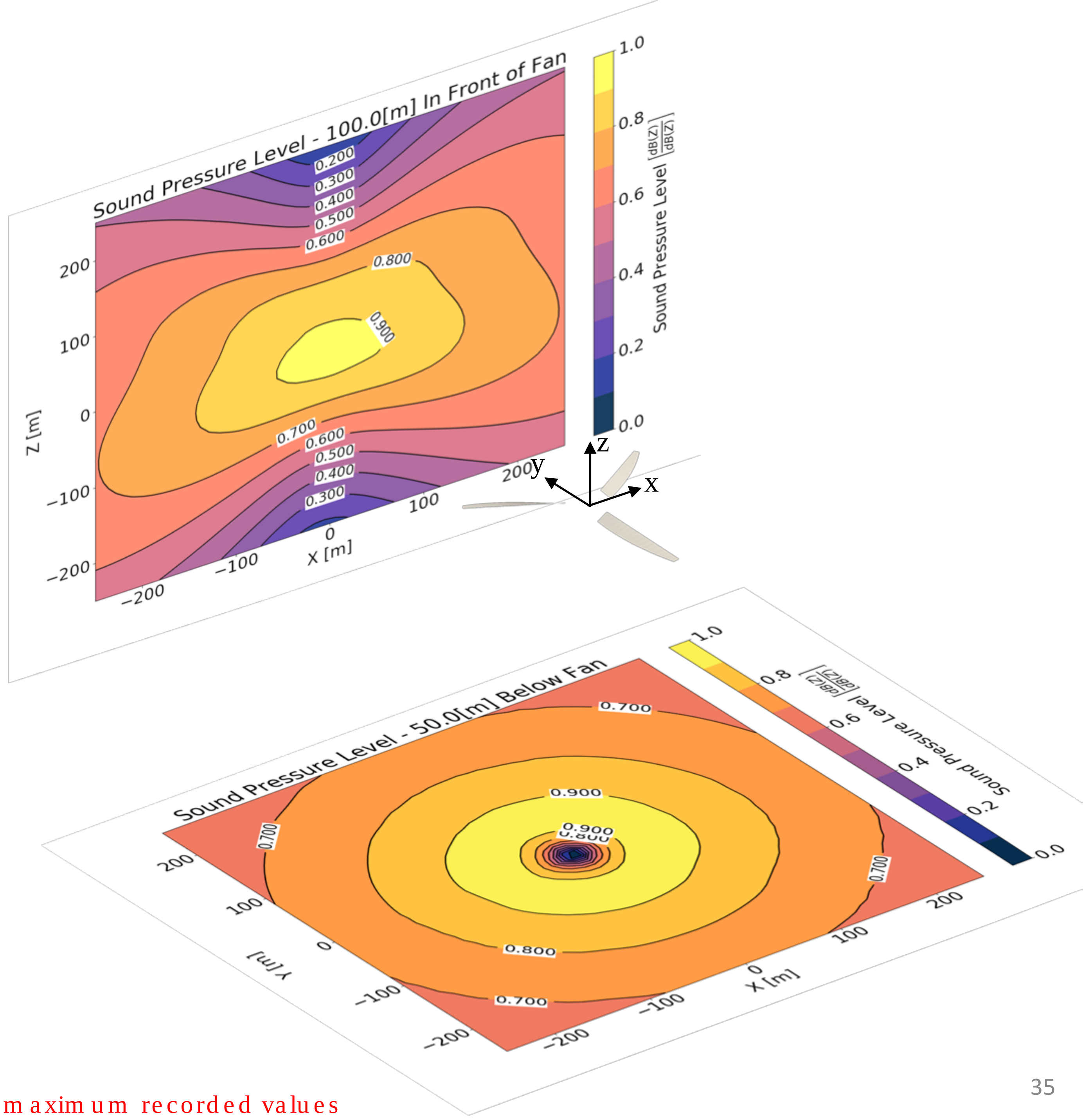

*Sound Pressure Level normalized to scale 0 – 1 between minimum and maximum recorded values

Two Fan Aerodynamic Analysis

Particle evolution and wake interaction in hover flight condition

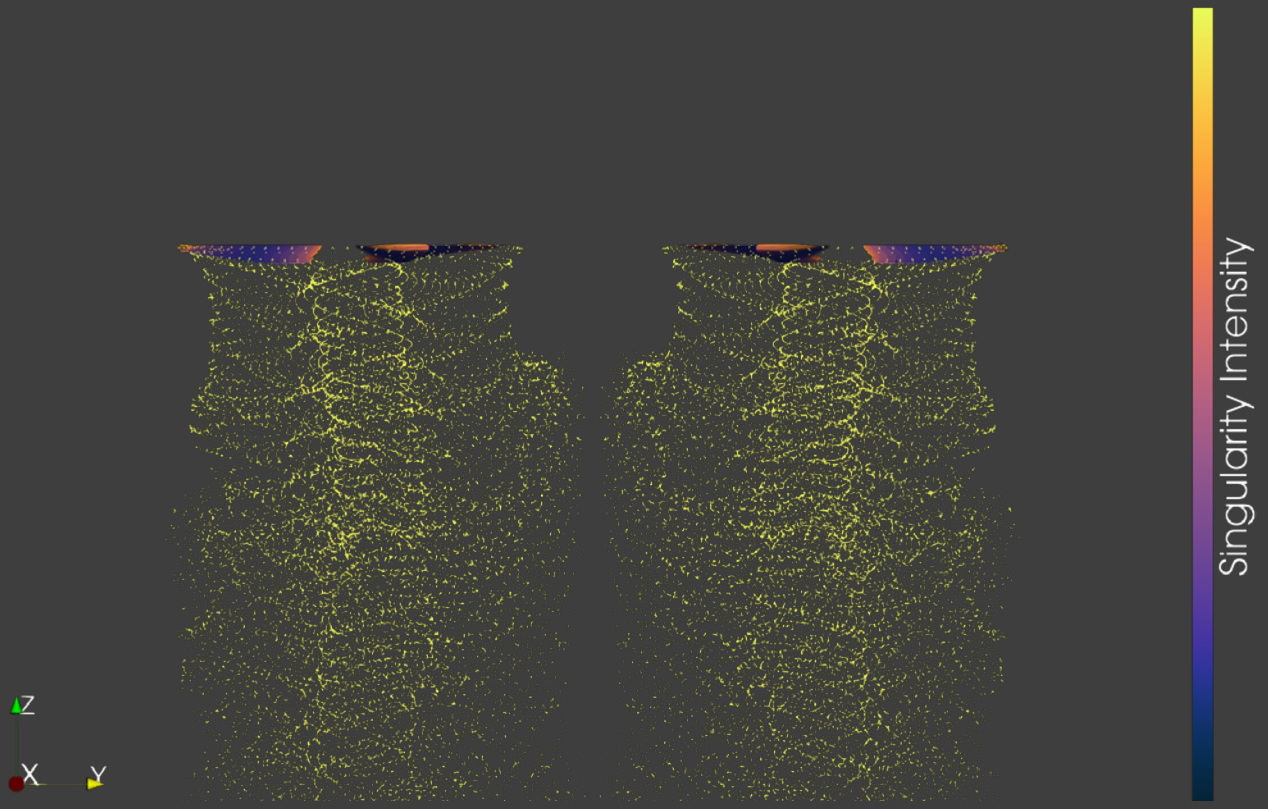

Cut plane of averaged velocity contours showing wake interaction in hover flight

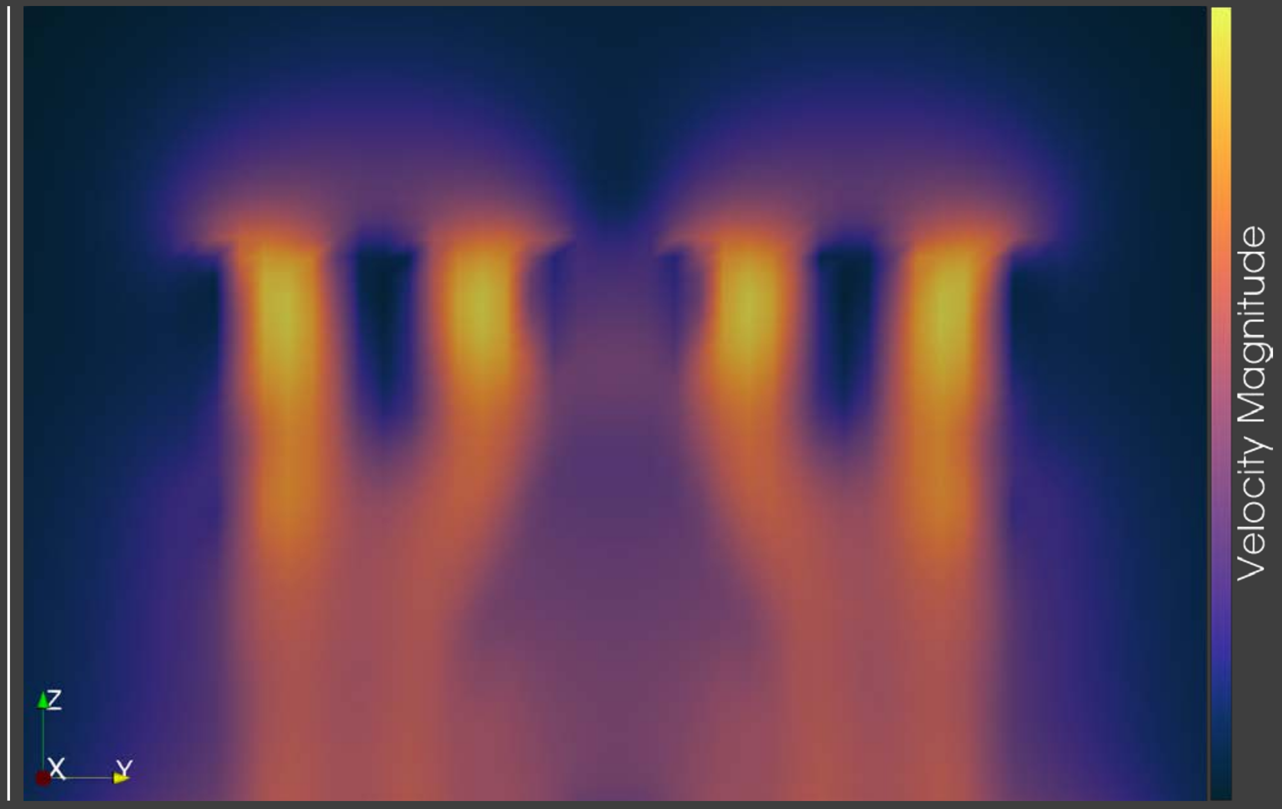

Two Fan Aeroacoustic Analysis

- Contour plot of Sound Pressure Level on plane below fans
- [X,Y,Z] = [-300, -300, -100] - [300 300, -100][m]
- Grid of [20 x 20] observer probes

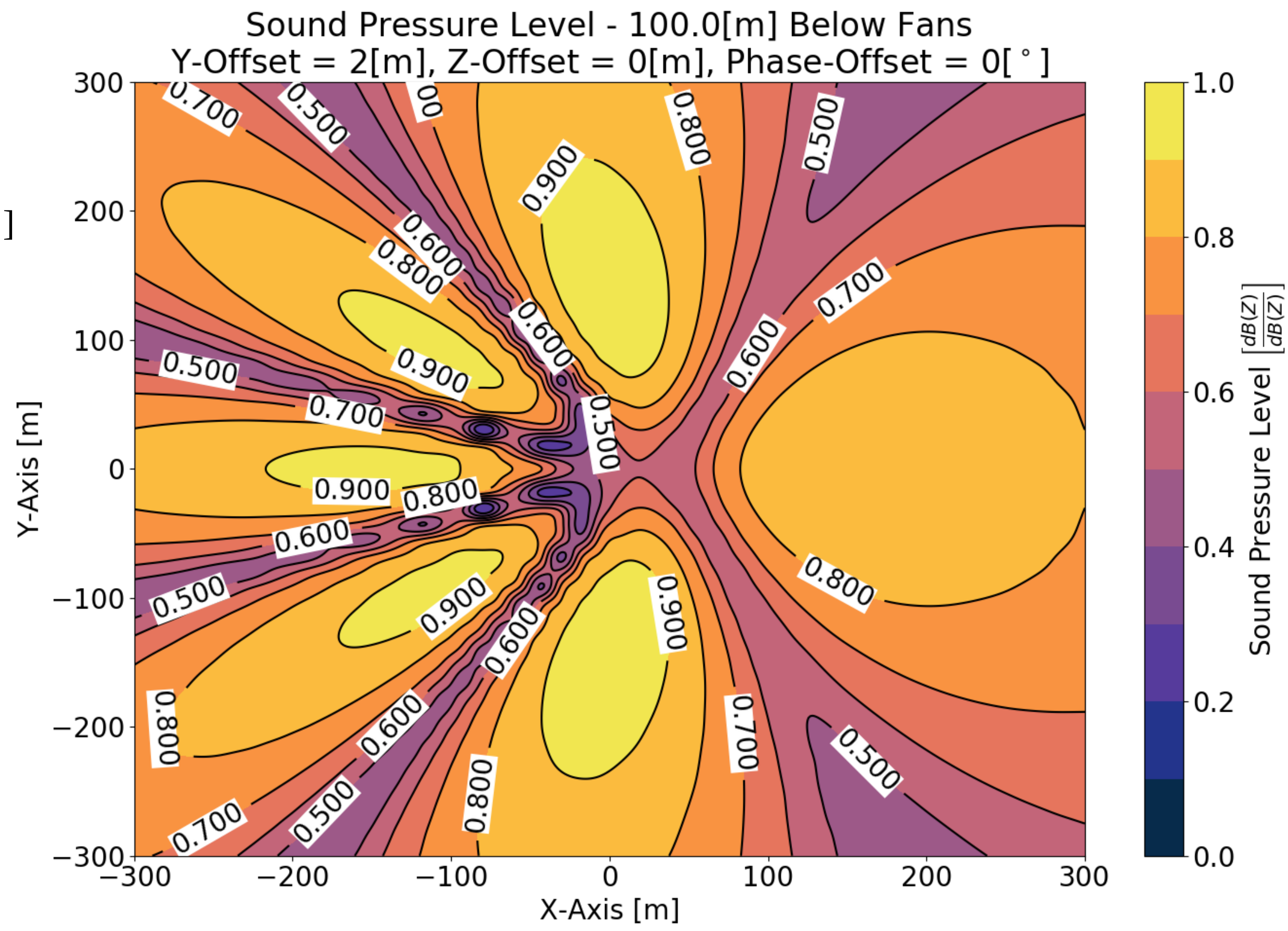

*Sound Pressure Level normalized to scale 0 – 1 between minimum and maximum recorded values

Parametric Study

- Study of the change in noise footprint with respect to horizontal, vertical, and phase offset between fans

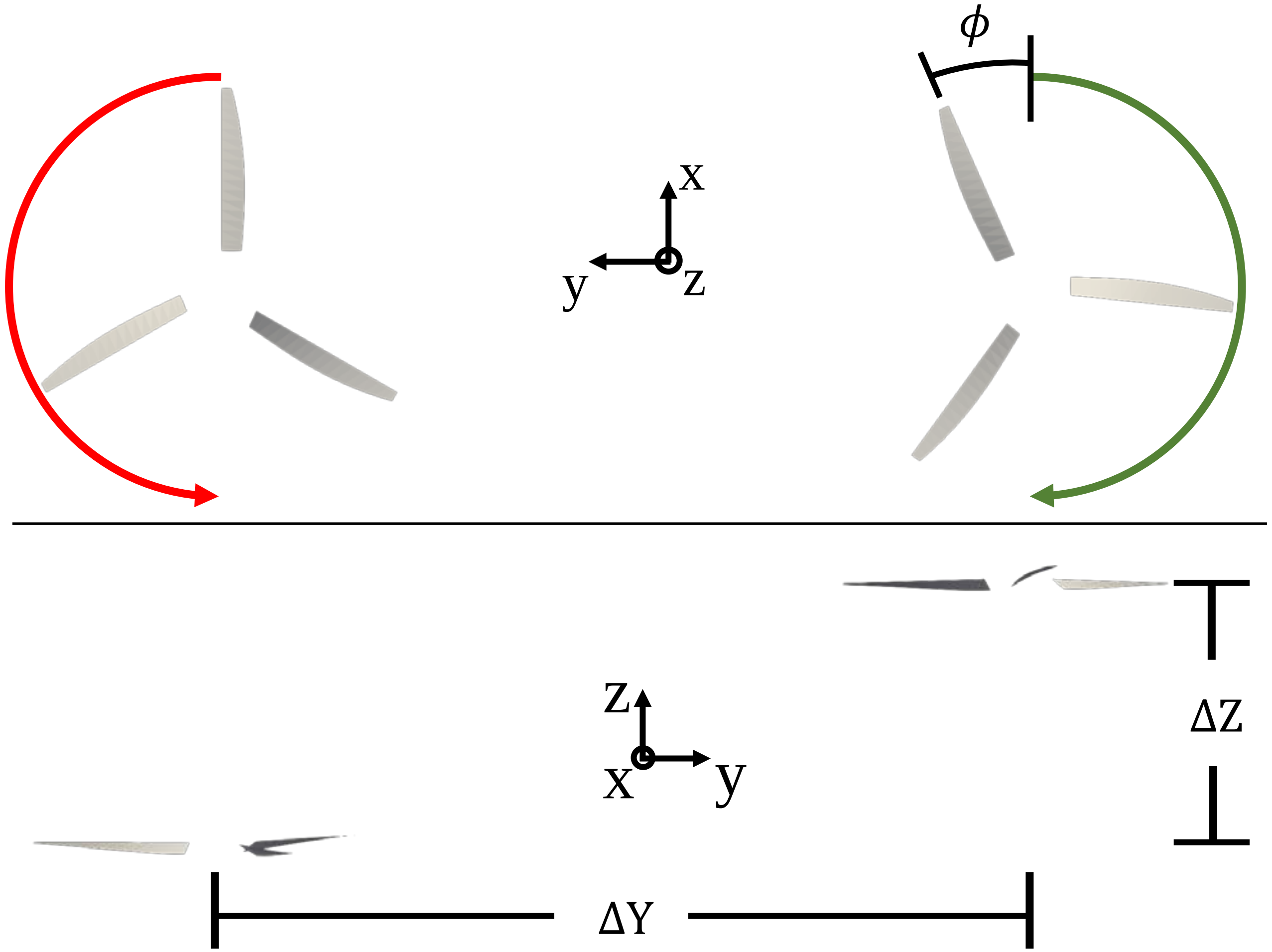

Case	Param.	Sampled Values	Units
Case 1	ΔY	$2.00, 2.50, 3.00, 3.50, 4.00$	$[m]$
	ΔZ	$0.00, 0.25, 0.50, 0.75, 1.00$	$[m]$
	ϕ	0.00	$[\circ]$
Case 2	ΔY	$2.00, 2.50, 3.00, 3.50, 4.00$	$[m]$
	ΔZ	0.00	$[m]$
	ϕ	$0, 24, 48, 72, 96$	$[\circ]$
Case 3	ΔY	3.00	$[m]$
	ΔZ	$0.00, 0.25, 0.50, 0.75, 1.00$	$[m]$
	ϕ	$0, 24, 48, 72, 96$	$[\circ]$

Parametric Study: Results

- Slices of the design space recording the average sound pressure level on the plane below the vehicle

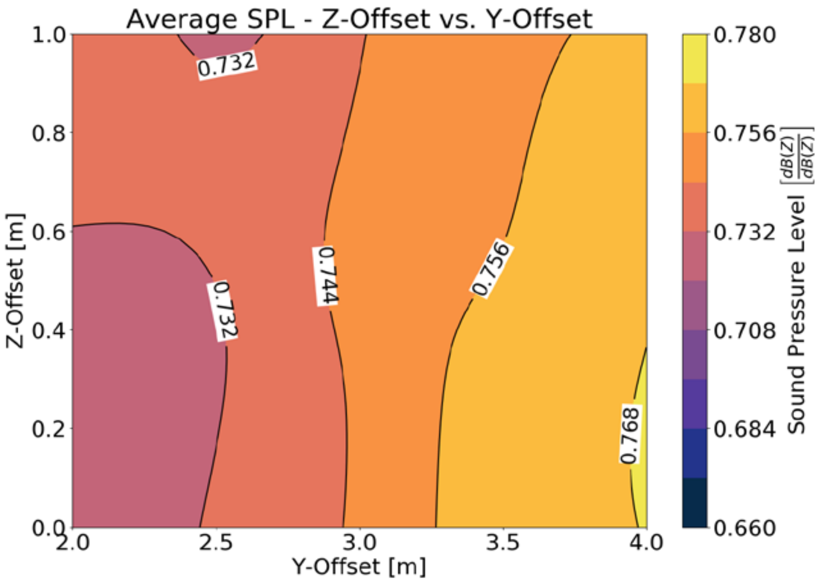

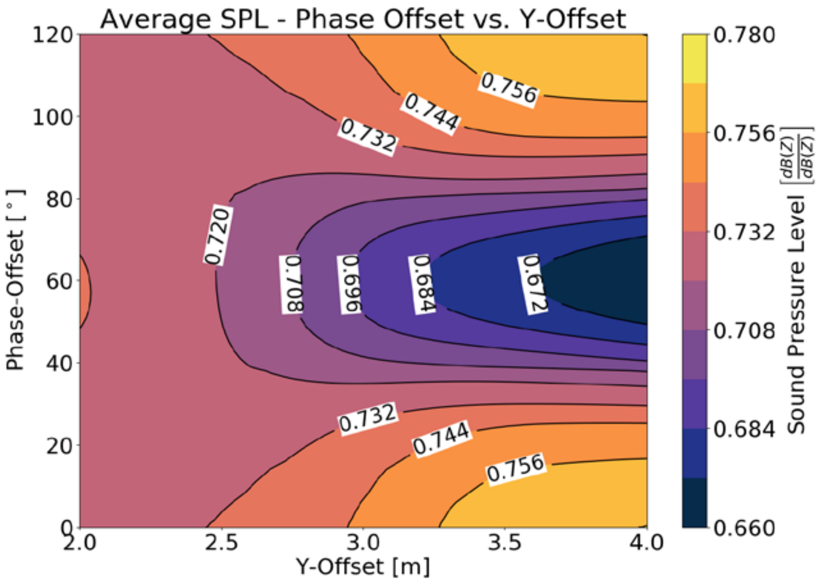

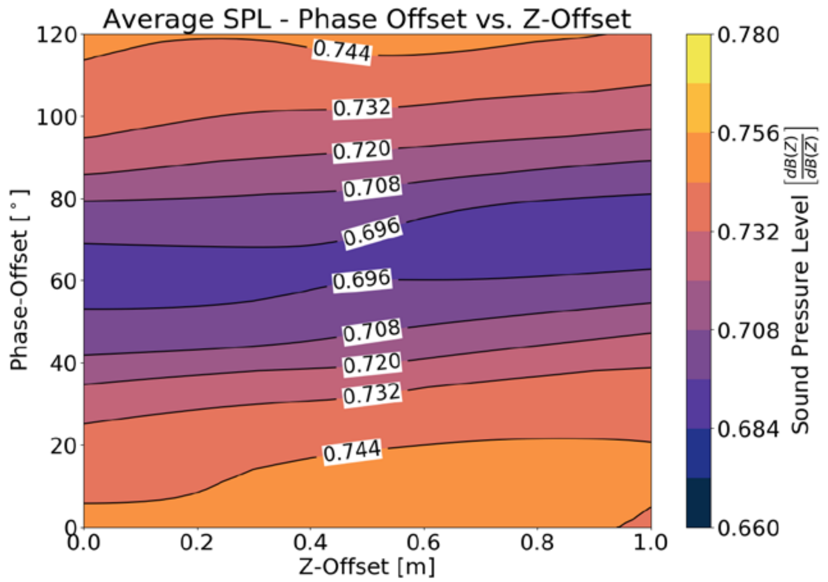

- Clear contours that show noise increases with increasing Y-offset
- Slight Z-offset dependence especially at low values of Y-offset

- Clear dependence on phase offset at large values of Y-offset
  - In phase: increased noise
  - Out of phase: decreased noise

- Phase offset has distinct effect
  - In phase: increased noise
  - Out of phase: decreased noise
- Z-offset has only minimal effect

→ Without even changing the rotor design or operating conditions, we can substantially change the noise footprint of multiple rotors in operation

*Sound Pressure Level normalized to scale 0 – 1 between minimum and maximum recorded values

Hybrid Blade Element Momentum Theory

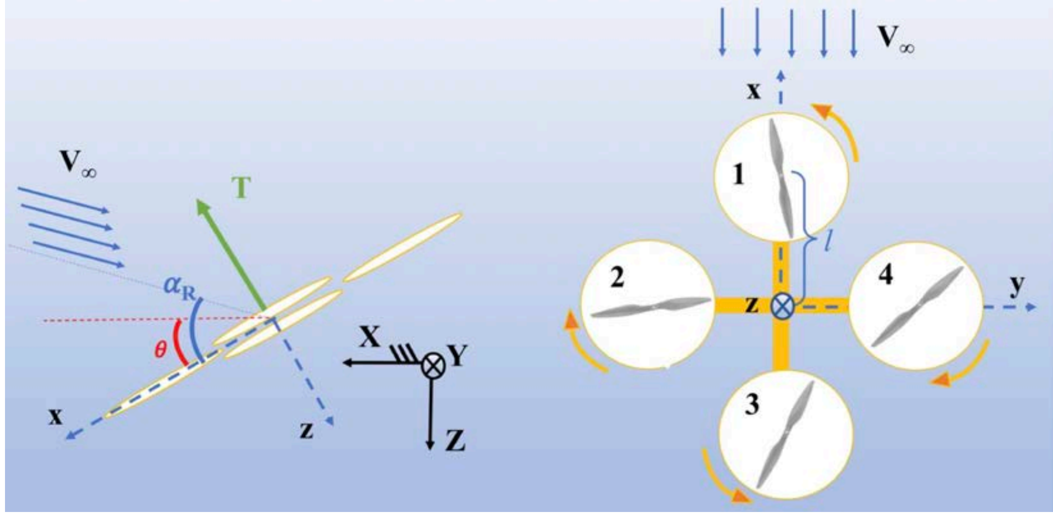

Momentum Theory C_T: $C_{T,MT} = \dfrac{T_{des}}{\pi \rho V_t^2 R^2}$

Inflow Ratio: $\lambda_0 = \lambda_c + \dfrac{C_T}{2\sqrt{\mu^2 + \lambda_0^2}}$ Where: $\mu = \dfrac{\sqrt{V_x^2+V_y^2}}{V_{tip}}$ and $\lambda_c = -\dfrac{V_z}{V_{tip}}$

=> Iteratively solve for λ_0 using Newton-Raphson method

Linear Inflow Model: $\lambda = \lambda_0(1 + k_x r\cos(\psi) + k_y r\sin(\psi))$ Where: $k_x = \frac{15\pi}{23}\tan\left(\frac{\chi}{2}\right)$; $k_y = 0$; $\chi = \tan^{-1}\left(\frac{\mu}{\lambda_0}\right)$

Coefficient of Lift:

For each cross-section at each azimuthal angle: $C_l = C_{l\alpha}\alpha_{eff}$

Stall Model:

Adjust C_l for each section using stall model:

$$C_l = (1-\sigma)C_{l\alpha}\alpha_{eff} + \sigma[2sign(\alpha_{eff} - \alpha_{L=0})\sin^2(\alpha_{eff} - \alpha_{L=0})\cos(\alpha_{eff} - \alpha_{L=0})]$$

$$\text{Where: } \sigma = \frac{1+e^{-M(\alpha_{eff}-\alpha_{L=0}-\alpha_0)}+e^{M(\alpha_{eff}-\alpha_{L=0}+\alpha_0)}}{\left[1+e^{-M(\alpha_{eff}-\alpha_{L=0}-\alpha_0)}\right]\left[1+e^{-M(\alpha_{eff}-\alpha_{L=0}+\alpha_0)}\right]}$$

Blade Element Theory C_T:

Integrate Lift over rotor disk for Thrust:

$$C_{T,BET} = \frac{N_b}{4R\pi^2}\int_{r_{min}}^{1}\int_0^{2\pi} C_l u^2 c(r)\cos(\phi)\, d\psi dr$$

$$\mathcal{R}(T_{\text{mag}}) = C_{T,BET}(T_{\text{mag}}) - C_{T,MT}(T_{\text{mag}}) \Rightarrow 0$$

Davoudi, B., and Duraisamy, K., “A Hybrid Blade Element Momentum Model for Flight Simulation of Rotary Wing Unmanned Aerial Vehicles,” AIAA Aviation Forum, Dallas, Texas, 2019, pp. 1–21. doi:10.2514/6.2019-2823.

Brent's Method

Bracket root of function $f(x)$ within domain a, b:

Repeat until $f(b \; or \; s) = 0$ or $|b - a|$ is small enough:

If $f(a) \neq f(c)$ and $f(b) \neq f(c)$ then:

Inverse Quadratic Interpolation:

$$s = \frac{af(b)f(c)}{\big(f(a) - f(b)\big)\big(f(a) - f(c)\big)} + \frac{bf(a)f(c)}{\big(f(b) - f(a)\big)\big(f(b) - f(c)\big)} + \frac{cf(a)f(b)}{\big(f(c) - f(a)\big)\big(f(c) - f(b)\big)}$$

Else:

Secant Method

$$s = b \; - f(b) \; \frac{b-a}{f(b)-f(a)}$$

If s is not between $\frac{3a+b}{4}$ and b or mflag is set and $|s - b| \geq \frac{|b-c|}{2}$ or mflag is cleared and $|s - b| \geq \frac{|c-d|}{2}$ or mflag is set and $|b - c| < |\delta|$ or mflag is cleared and $|c - d| < |\delta|$:

Bisection Method

$$s = \frac{a+b}{2}; \text{ Set mflag}$$

Else:

Clear mflag

Bracket root using linesearch starting at $x = 0$ and searching for change in sign of residual function

Brent, R. P., Algorithms for Minimization without Derivatives, Prentice-Hall, Englewood Cliffs, NJ, 1973.

Compact Aeroacoustic Formulation

- Elements such as lifting-lines and flat plates can be reconstructed using a compact source-sink method
  - A source-sink pair is ’placed’ at each discretized airfoil section to mimic the actual airfoil geometry

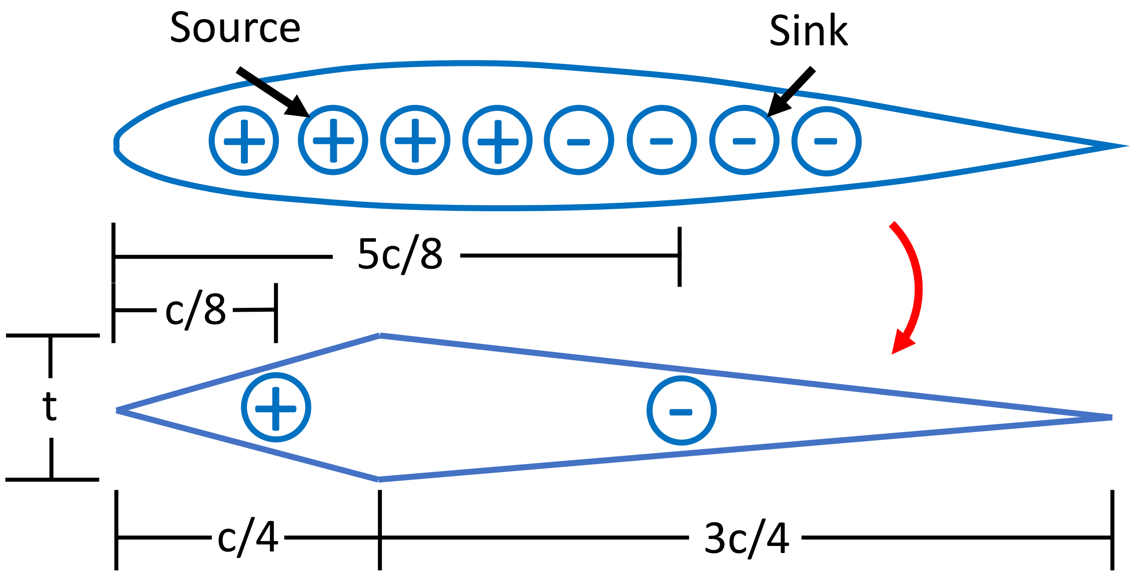

Modified monopole (thickness) pressure perturbation equation based on source-sink method

$$p'_T(\vec{x},t) = \frac{1}{4\pi}\left[\frac{\rho_0 \dot{u}_0 t dS}{r(1-M_r)^2}\right]\Bigg|_{Source,\tau^*} + \frac{1}{4\pi}\left[\frac{-\rho_0 \dot{u}_0 t dS}{r(1-M_r)^2}\right]\Bigg|_{Sink,\tau^*}$$
$$+ \frac{1}{4\pi}\left[\frac{\rho_0 u_0 t dS\left(r\dot{M}_i\hat{r}_i + a_0(M_i\hat{r}_i - M_iM_i)\right)}{r^2(1-M_r)^3}\right]\Bigg|_{Source,\tau^*}$$
$$+ \frac{1}{4\pi}\left[\frac{-\rho_0 u_0 t dS\left(r\dot{M}_i\hat{r}_i + a_0(M_i\hat{r}_i - M_iM_i)\right)}{r^2(1-M_r)^3}\right]\Bigg|_{Sink,\tau^*}$$

F H Schmitz and Y H Yu. Helicopter Impulsive Noise: Theoretical and Experimental Status. Technical report, NASA Ames Research Center, Moffett Field, California, 1983.

Airfoil Sectional Data

- Simulated baseline hover operating condition at each airfoil section
- Viscous formulation with $0.1°$ analysis steps
- Values needed for Hybrid Blade Element Momentum Theory model:
    - Lift-curve slopes ($C_l \ vs. \alpha$) values
    - Stall onset angle of attack
- Sections 3 & 4 are more challenging to converge – assumed to stall approximately where XFoil fails to converge

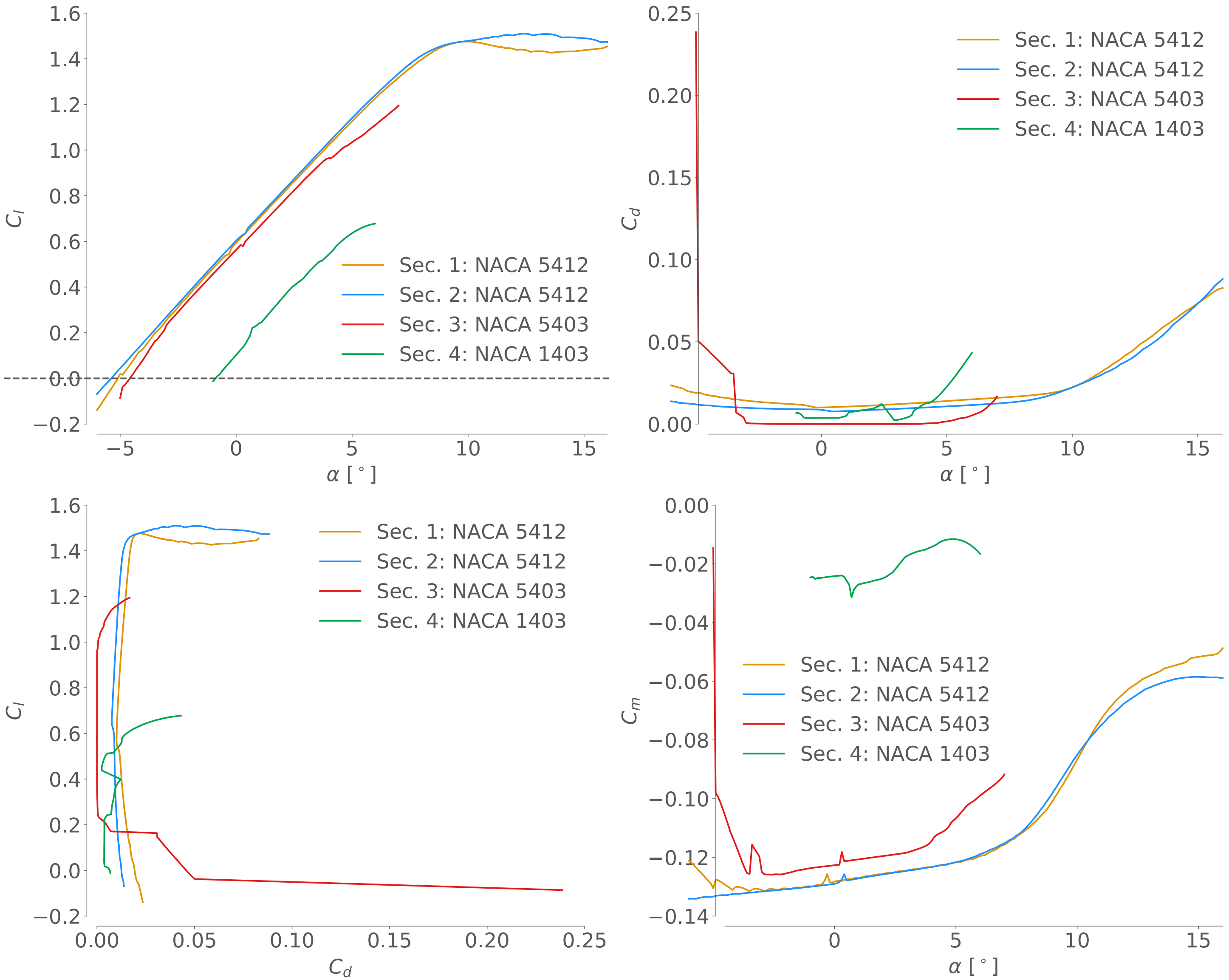

Quadrotor Optimization: Rotor Data

- Rotor blade data defined at radial locations along span, obtained from OpenVSP model
  - Four airfoil sections, interpolated across span
- Airfoil sections simulated using pyXLIGHT / XFoil in hover flight condition ($\omega = 75\, rad/s$)

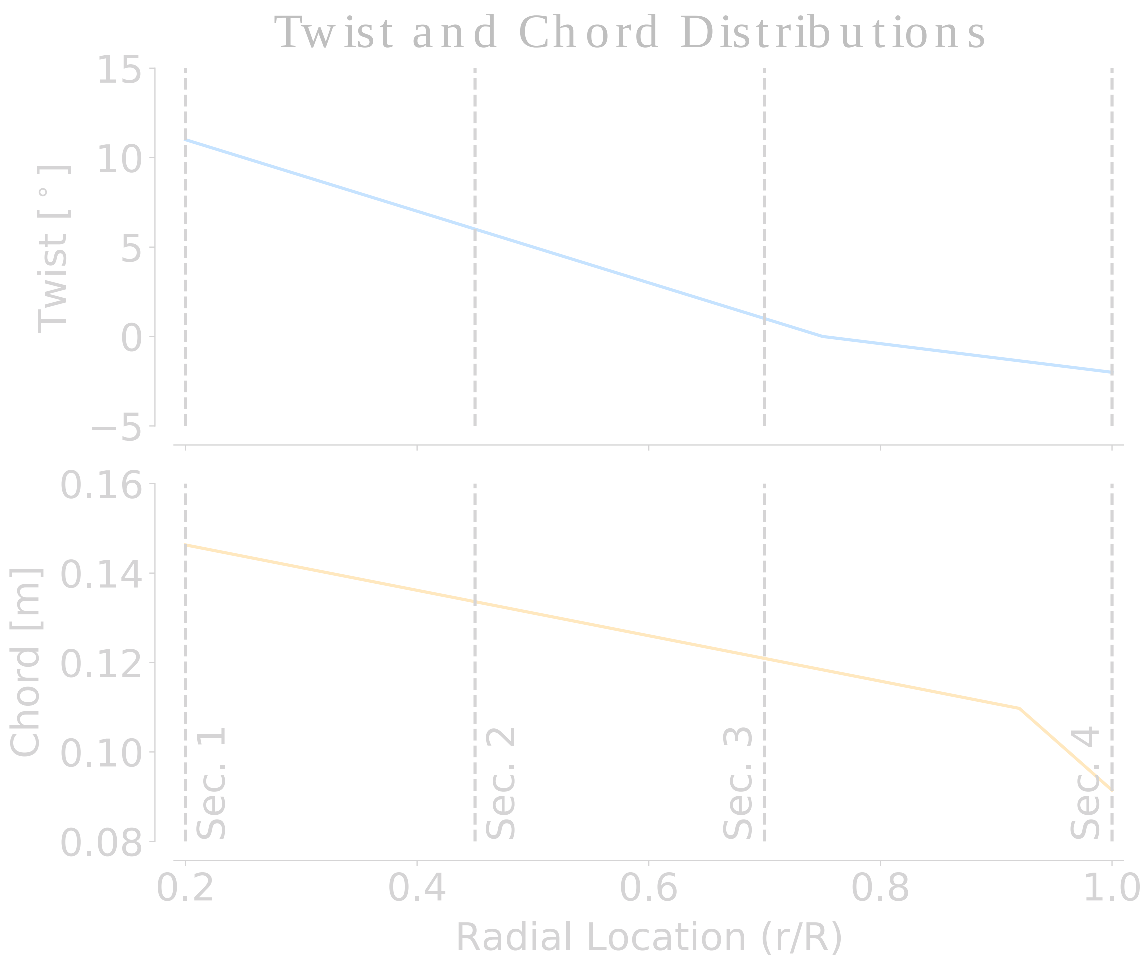

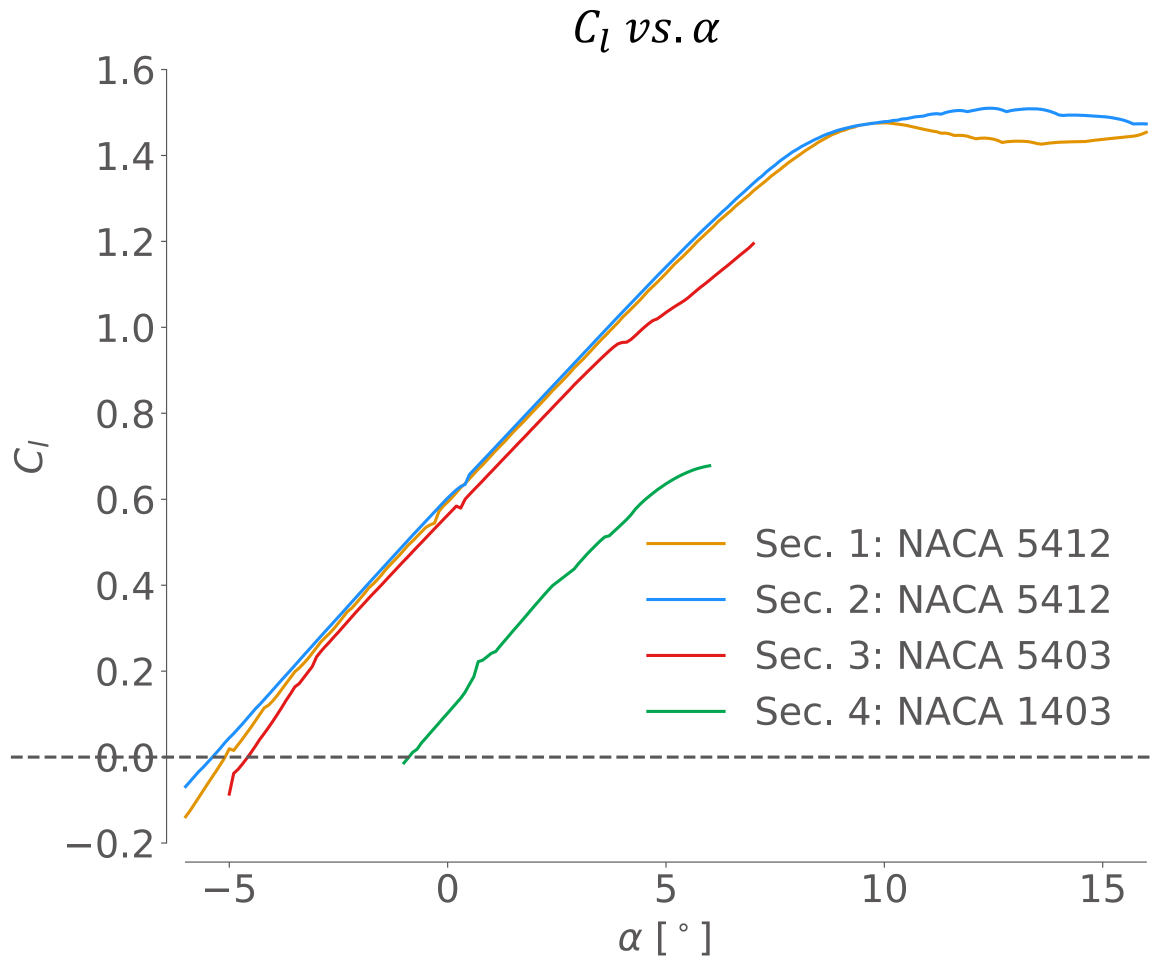

Kreisselmeier-Steinhauser (KS) Aggregation

- Minimizing a maximum value can be challenging as it may be discontinuous

- The Kreisselmeier-Steinhauser (KS) function aggregates all of the recorded values and smooths the design space so the overall function is continuous

- Each independent function, $g_j(x)$, is aggregated using an aggregation parameter, ρ, in the equation below:

$$KS\left(g_j(x)\right) = \frac{1}{\rho}\log_e\left(\sum_{i}^{n_g} e^{\rho g_j(x)}\right)$$

- $KS\left(g_j(x)\right)$ represents the maximum function value that can be constrained or minimized

Kreisselmeier, G., and Steinhauser, R., "Systematic Control Design by Optimizing a Vector Performance Index," IFAC Proceedings Volumes, Vol. 12, No. 7, 1979, pp. 113–117. doi:10.1016/s1474-6670(17)65584-8, URL http://dx.doi.org/ 10.1016/S1474-6670(17)65584-8.